

DESIGN AND IMPLEMENTATION OF A ROBOT-ASSISTED REHABILITATION
SYSTEM, REHABROBY

by
Fatih ÖZKUL

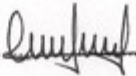
Submitted to the Institute of Graduate Studies in
Science and Engineering in partial fulfillment of
the requirements for the degree of
Master of Science
in
Electrical and Electronics Engineering

Yeditepe University
2011

DESIGN AND IMPLEMENTATION OF A ROBOT-ASSISTED REHABILITATION
SYSTEM, REHABROBY

APPROVED BY:

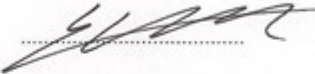
Assist. Prof. Dr. Duygun Erol Barkana
(Supervisor)


.....

Prof. Dr. Serap Inal


.....

Assoc. Prof. Dr. Cem Ünsalan


.....

DATE OF APPROVAL:/...../.....

ACKNOWLEDGEMENTS

I am heartily thankful to my supervisor, Asst. Prof. Dr. Duygun Erol Barkana for her encouragement, guidance and patience throughout the development of this thesis. It is a pleasure to thank to my thesis committee members Prof. Dr. Serap İnal and Assoc. Prof. Dr. Cem Ünsalan and also I would like to thank to Asst. Prof. Dr. Şule Badilli Demirbaş for their instructive comments and suggestions. Finally, I would like to special thanks to Dr. Seda Arslan and to my family for their patient love and support.

This study was supported by the Support Programme for Scientific and Technological Research Projects (TÜBİTAK-3501) under Grant 108E190.

ABSTRACT

DESIGN AND IMPLEMENTATION OF A ROBOT-ASSISTED REHABILITATION SYSTEM, REHABROBY

In recent years, robot-assisted rehabilitation systems have become an active research area to quantitatively monitor and adapt to patient progress, and to ensure consistency during the rehabilitation. In this thesis, an exoskeleton type robot-assisted rehabilitation system called RehabRoby is developed for upper extremity rehabilitation purposes. A control architecture, which contains a high-level controller and a low-level controller, is designed for RehabRoby to complete the rehabilitation task in a desired and safe manner. A hybrid system modeling technique is used for high-level controller. An admittance control with inner robust position control loop is used for the low-level control of RehabRoby. Real-time experiments are performed with healthy subjects to evaluate control architecture of the robot-assisted rehabilitation system RehabRoby. Furthermore, usability of RehabRoby has been evaluated during the execution of rehabilitation tasks.

ÖZET

ROBOT DESTEKLİ BİR REHABİLİTASYON SİSTEMİ REHABROBY' NİN TASARIMI VE UYGULAMASI

Son yıllarda robot destekli rehabilitasyon sistemleri niceliksel gözlem, hasta gelişimine adapte olma ve rehabilitasyon süresince tutarlılığı sağlama özellikleri itibariyle aktif bir araştırma alanı haline gelmiştir. Bu tezde üst uzuvların rehabilitasyonu amacıyla RehabRoby adlı eksoskeleton tip bir robot destekli rehabilitasyon sistemi geliştirilmiştir. RehabRoby'nin rehabilitasyon görevlerini istenilen ve güvenli bir şekilde gerçekleştirmesini sağlayacak, içerisinde üst-düzey ve alt-düzey denetçileri barındıran bir kontrol mimarisi tasarlanmıştır. Üst-düzey denetçi tasarımında hibrit sistem modelleme tekniğinden yararlanılmıştır. RehabRoby'nin alt-düzey denetçi tasarımında dayanıklı pozisyon kontrol iç döğüsünü içeren admitans kontrol yöntemi kullanılmıştır. Robot destekli rehabilitasyon sistemi RehabRoby'nin kontrol mimarisini değerlendirmek amacıyla sağlıklı denekler ile gerçek zamanlı deneyler gerçekleştirilmiştir. Ayrıca RehabRoby'nin rehabilitasyon görevleri esnasında kullanılabilirliği test edilmiştir.

TABLE OF CONTENTS

ACKNOWLEDGEMENTS.....	iii
ABSTRACT.....	iv
ÖZET	v
TABLE OF CONTENTS.....	vi
LIST OF FIGURES	viii
LIST OF TABLES.....	xi
LIST OF SYMBOLS / ABBREVIATIONS.....	xii
1. INTRODUCTION	1
2. BACKGROUND	3
2.1. MECHANICAL DESIGN OF ROBOT ASSISTED REHABILITATION	
SYSTEMS FOR UPPER EXTREMITIES	3
2.1.1. End-Effector Based Arm Rehabilitation Robots.....	4
2.1.2. Exoskeleton Type Arm Rehabilitation Robots	7
2.2. CONTROL OF ROBOT-ASSISTED REHABILITATION SYSTEMS.....	
FOR UPPER EXTREMITIES	10
3. METHODOLOGY	12
3.1. CONTROL ARCHITECTURE	12
3.2. DESIGN OF REHABROBY	12
3.3. SENSORS AND CONTROL HARDWARE OF REHABROBY.....	19
3.4. CONTROLLERS OF REHABROBY	21
3.4.1. Low Level Controller.....	22
3.4.2. High Level Controller	29
4. EXPERIMENTAL RESULTS	31
4.1. EXPERIMENTAL PROTOCOL.....	31
4.2. RESULTS	33
5. CONCLUSION.....	41
APPENDIX A: BASIC SPECIFICATIONS OF MOTORS, DRIVERS AND.....	
GEAR UNITS USED IN REHABROBY	44

APPENDIX B: TECHNICAL DATA OF HUMUSOFT MF624 DATA	
ACQUISITION BOARD.....	46
APPENDIX C: CATALOG INFORMATION OF FORCE SENSOR AND	
CHARGE AMPLIFIER.....	47
APPENDIX D: TECHNICAL DATA OF THE MICROCONTROLLER	
(PIC16F877A) USED IN THE MICROCONTROLLER CIRCUIT ..	49
APPENDIX E: PROGRAM CODE USED IN THE MICROCONTROLLER	50
REFERENCES	53

LIST OF FIGURES

Figure 2.1.	MIT-Manus.....	4
Figure 2.2.	MIME	5
Figure 2.3.	GENTLE/s.....	6
Figure 2.4.	NEuroREhabilitationroBOT (NeReBot)	6
Figure 2.5.	ARMin II	7
Figure 2.6.	ARMin III.....	8
Figure 2.7.	T-WREX.....	9
Figure 2.8.	L-Exos	9
Figure 2.9.	SRE.....	10
Figure 3.1.	Control architecture of RehabRoby.....	12
Figure 3.2.	Rehabilitation movements for upper extremities	14
Figure 3.3.	RehabRoby's axes	15
Figure 3.4.	RehabRoby system with subject.....	16
Figure 3.5.	Adjustable link lengths and height of RehabRoby	17
Figure 3.6.	RehabRoby with counterweight system	18

Figure 3.7. Transition steps of RehabRoby for left arm use	19
Figure 3.8. Placement of the force sensors	20
Figure 3.9. General data flow in the control hardware	21
Figure 3.10. Block diagram of low-level controller of RehabRoby	23
Figure 3.11. Block diagram of the robust position controller	29
Figure 3.12. Block diagram of the high-level controller of RehabRoby	30
Figure 4.1. Subject with RehabRoby during tasks	32
Figure 4.2. Robust position controller without disturbance estimator	34
Figure 4.3. Robust position controller with disturbance estimator	35
Figure 4.4. Visual feedback	36
Figure 4.5. Motion of S4 during Task1 in AAT	37
Figure 4.6. Motion of S4 during Task1 in RAT	37
Figure 4.7. Motion of S4 during Task2 in AAT	38
Figure 4.8. Motion of S4 during Task2 in RAT	39
Figure A.1. Specifications of the motor drivers	45
Figure B.1. Humusoft MF624 data acquisition board	46

Figure C.1. Technical data of the force sensor	47
Figure C.2. Technical data of the charge amplifier	48
Figure D.1. Pin diagram of the PIC16F877A microcontroller	49

LIST OF TABLES

Table 3.1.	Motion specifications of RehabRoby	15
Table 4.1.	The position controller parameters and RehabRoby model parameters.....	34
Table 4.2.	Position errors of each subject for both Task1 and Task2.....	39
Table 4.3.	The number of times assistance.....	40
Table 4.4.	Questionnaire results for the assessment of the use of RehabRoby	40
Table A.1.	Basic specifications of motors used in the axes of RehabRoby	44
Table A.2.	Rating table of gear units of RehabRoby	45

LIST OF SYMBOLS / ABBREVIATIONS

A_i	System matrix of the i th joint
baud	Baud rate
B_d	Desired viscosity coefficient matrix in admittance filter
B_i	Control input vector for the i th joint
$b(\dot{q})$	Friction force vector
B_v	Viscous-friction coefficient vector
C_i	Output matrix for the i th joint
d	Total equivalent disturbance
d'	Equivalent disturbance vector
d_i	Equivalent disturbance for the i th joint
\hat{d}_i	Estimated value of the equivalent disturbance in the i th joint
deg	Degree
deg/sec	Degree/second
e	Emergency stop flag
E_i	Disturbance vector for the i th joint
G_i	Kalman gain matrix for the i th joint
$G(q)$	Gravity force vector
i_{ci}	Feed forward compensating current signal for the i th joint
i_{di}	Compensating current signal for the i th joint
i_r	Current reference of the motor
i_{ri}	Motor current reference of the i th joint
K_i	State feedback gain matrix for the i th joint
K_d	Desired stiffness coefficient matrix in admittance filter
k_{di}	Derivative gain calculated for the i th joint
k_{gr}	Gear ratio of the actuator
k_{pi}	Proportional gain calculated for the i th joint
k_t	Nominal value of the motor torque constant
K_{tr}	Diagonal matrix that is calculated by multiplication of k_t and k_{gr}
L1	Adjustable upper arm length value of RehabRoby

L_2	Adjustable lower arm length value of RehabRoby
L_3	Adjustable height value of RehabRoby
\bar{M}	Diagonal matrix that includes constant diagonal terms of $M(q)$
M_d	Desired inertia matrix in admittance filter
$M(q)$	Manipulator inertia tensor matrix
Nm	Newton meter
P_i	Covariance matrix of the estimation errors for the i th joint
P_i^-	Priori estimate of the covariance matrix for the i th joint
q_s	Joint position vector
\dot{q}	Joint velocity vector
\ddot{q}	Joint acceleration vector
q_i	Position of the i th joint
Q_i	Covariance matrix of the model errors for the i th joint
\dot{q}_i	Velocity of the i th joint
q_r	Reference joint position vector
\dot{q}_r	Reference joint velocity vector
\ddot{q}_r	Reference joint acceleration vector
R_i	Covariance scalar of measurement errors for the i th joint
T	Characteristic time constant
T_s	Sampling time
u_{di}	Equivalent disturbance in the state space model of the i th joint
u_i	Control input (motor current reference) of the i th joint
v_i	Measurement noise in the i th joint
$V(q, \dot{q})$	Coriolis and centrifugal forces vector
x_i	State vector of the i th joint
y_i	Measured output in the i th joint
$\Delta b(\dot{q})$	Vector that includes nonlinear and uncertain terms of $b(\dot{q})$
$\Delta M(q)$	Matrix that includes nonlinear and uncertain terms of $M(q)$
$\Delta \tau$	Vector that includes variations of the applied joint torque
ε	Error limit
θ	Vector of angles of the joints of RehabRoby

θ_1	Angle of horizontal abduction/adduction of shoulder rotation axis
θ_2	Angle of shoulder flexion/extension elevation
θ_3	Angle of internal and external rotation of shoulder axis
θ_4	Angle of elbow flexion/extension axis
θ_5	Angle of lower arm elbow pronation/supination axis
θ_6	Angle of wrist flexion/extension axis
ξ	Damping ratio
τ	Joint torque vector
τ_a	Applied torque in admittance filter
ω_0	Natural frequency

AAT	Active-assisted therapy
ADL	Activities of daily living
DoF	Degrees of freedom
IRB	Institutional Review Board
L-Exos	Light Exoskeleton
LKF	Linear Kalman filter
MIME	Mirror Image Movement Enabler
NeReBot	NEuroREhabilitationroBOT
PIC	Programmable interface controller
PID	Proportional-Integral-Derivative
Pneu-Wrex	Pneumatic Wilmington Robotic Exoskeleton
RAT	Resistive-assisted therapy
RoM	Range of motion
Rs232	Recommended Standard 232
S	Subject
SRE	Salford Rehabilitation Exoskeleton
T-Wrex	Therapy Wilmington Robotic Exoskeleton

1. INTRODUCTION

There are over 650 million people around the world with disabilities. Although it is accepted as 10% of the whole world population, it is 15.7% in Europe, 12% in USA and 12.29% in Turkey [1]. Physical disability, which occurs by birth or acquired during the life span of the person due to the diseases or a trauma to the central nervous system or musculoskeletal system, affects the functionality of people. The physical therapy programs are applied to people with disability to increase their joint range, strength, power, flexibility, coordination and agility of the person, and to improve their functional capacity [2,3]. The availability of such therapy programs, however, is limited by a number of factors such as the amount of costly therapist's time they involve and the ability of the therapist to provide controlled, quantifiable, and repeatable assistance to complex movement. Consequently, robot-assisted rehabilitation that can quantitatively monitor and adapt to patient progress, and ensure consistency during rehabilitation may provide a solution to these problems and has become an active research area [4-12].

Robot-assisted rehabilitation systems have been developed for upper, lower or both upper and lower extremities. This thesis presents an upper extremity robot-assisted rehabilitation system. There are two kinds of robot-assisted rehabilitation systems for upper extremities in terms of mechanical design which are end-effector based and exoskeleton type rehabilitation robots. MIT-MANUS [4], MIME [5], GENTLE/S [6] and NeReBot [7] are end-effector based and ARMin [8], T-WREX [9], Pneu-WREX [10], L-Exos [11] and Salford Rehabilitation Exoskeleton [12] are exoskeleton type robot-assisted rehabilitation systems. Exoskeleton type robots resemble the human arm anatomy and each joint of robot can be controlled separately, which reduces control issue complexity. In this thesis, an exoskeleton type upper-extremity robot-assisted rehabilitation system, which is called RehabRoby, is developed. RehabRoby has been designed in such a way that i) it can implement passive, active-assisted and resistive-assisted therapy modes, ii) it can be easily adjustable for people with different heights and arm lengths, and iii) it can be used for both right and left arm rehabilitation.

Note that control of RehabRoby in a desired and safe manner is an important issue. Impedance control [4,7,8,11,12] admittance control [5-8], position control [5] and force control [10] have previously been used in the control of the upper extremity robot-assisted rehabilitation systems. There is a human-robot interaction in the robot-assisted rehabilitation systems, which is an external effect that can cause changes in the dynamics of the robotic systems. The changes in the dynamics of the robot may result in instability, which may affect the tracking performance. Therefore, a controller which is independent of dynamic model of robot-assisted system is needed for RehabRoby to compensate changes in the dynamics of the robotic system [13]. In this thesis, admittance control with inner robust position control loop is used to control RehabRoby in a desired manner. Note that it is also desirable for a patient to perform the rehabilitation task in a safe manner. A high-level controller, which is a decision making mechanism, is designed to ensure safety during the execution of the rehabilitation task. The high-level controller presented in this thesis plays the role of a human supervisor (therapist) who would otherwise monitor the task and assess whether the rehabilitation task needs to be updated.

In this thesis, the control architecture of RehabRoby has been evaluated performing two well-known rehabilitation tasks (elbow flexion and elbow flexion with shoulder flexion) with healthy subjects in active-assisted and resistive-assisted therapy modes. The results of these evaluations may provide us clues about the efficacy of RehabRoby for rehabilitation of upper extremity movements, usability of the RehabRoby and availability of use of RehabRoby for stroke patients.

In this thesis, background of robot-assisted rehabilitation systems is presented in Chapter 2. The control architecture, design specifications, hardware and controllers of RehabRoby are given in Chapter 3. The experimental results of RehabRoby system are presented in Chapter 4. Conclusion of the thesis and plans for future work are given in Chapter 5.

2. BACKGROUND

Rehabilitation robotics has been an active research area since 1985. The first publication in the field of rehabilitation robotics was about MIT-MANUS [4]. Robot supported physical therapy systems first used in large scaled clinical tests in 1998 and till today several robot-aided rehabilitation systems have been developed [14,15].

Robot-aided rehabilitation systems can be grouped into two classes. One consists of home-use systems that help patients in activities of daily living (ADL). These systems are used only for a single patient such as wheelchairs, mobile service robots, assistive manipulators that can be mounted onto wheelchairs or desks. The other one is the therapeutic systems that are used in clinical environment and they are shared by several patients [8].

In this thesis, we develop a rehabilitation robotic system that can be grouped in therapeutic systems. Therapeutic systems are also grouped into three classes: passive, active and interactive. In passive systems, there is no actuator and patient limbs are provided to make stable and limited movements. In active systems, there are actuators that drive patient limbs. Generally in active systems open-loop control or simple position control are used to drive the patient limb to the desired positions to complete the therapy tasks. Interactive systems are based on patient-robot interaction; torques and forces applied by the patients are measured by force-torque sensors and feedback to the system during the interaction. Impedance or admittance control strategies are used in interactive system to modify the robot motion according to patient's movement capabilities.

2.1. MECHANICAL DESIGN OF ROBOT ASSISTED REHABILITATION SYSTEMS FOR UPPER EXTREMITIES

Existing therapeutic systems for upper extremities either provide a therapy that focuses multiple joint movements to perform activities of daily living (ADL) tasks or provide a therapy that focuses only on a single joint movement [8]. End-effector based or exoskeleton type robots have been previously used to help patients to perform ADL tasks

in therapy. The end-effector based robot is connected to the patient limb from one point (hand or forearm). The exoskeleton type robot is connected to the patient's arm from multiple points to resemble the kinematic structure of the arm. Human-robot connection is achieved at one point as: hand or forearm in end-effector based robots. The technical rotation axes and the number of DoF (degrees of freedom) of the robot can be selected arbitrary and independent of the human arm anatomy. Thus, the mechanical design and construction of end-effector based robots are much easier [16]. However, exoskeleton type robots resemble the human arm anatomy and the technical rotation axes of the robot must correspond to the rotation axis of the human joints [17]. Thus, end-effector based robots have more complex mechanical designs compared to exoskeleton type robots. On the other hand, in exoskeleton type robots, the arm posture is fully determined and each joint torque can be controlled separately. This reduces control issue complexity and hyperextensions can be avoided mechanically. We chose to design an exoskeleton type robot-assisted rehabilitation system to be able to move each joint of the arm separately.

2.1.1. End-Effector Based Arm Rehabilitation Robots

MIT-Manus, the pilot rehabilitation robotic system, has been developed in MIT in the early 1990's [4]. It provides two dimensional movements of the patient's hand. The end-effector of MIT-Manus is the robot-mounted handle gripped by the patient and forces and movements can be applied to the system using this handle (Figure 2.1). MIT-Manus is shown in Figure 2.1.



Figure 2.1. MIT-Manus

Mirror Image Movement Enabler (MIME) robot-aided system which is shown in Figure 2.2, has been developed with the cooperation of Stanford University and Veterans Affairs Palo Alto Health Care System [5]. Patients can achieve three dimensions ADL movements during the therapy with MIME system. MIME mechanism is composed of a PUMA 560, a six degrees of freedom (DoF) industrial robot manipulator and a hand-attachment in the end-effector. The forearm of the patient can be positioned within a large range of spatial positions and orientations with this mechanism. The position values that are obtained from the intact arm are given to the effected arm using a digitizer connection. It is possible to execute passive, active, and active limited therapy methods using MIME.



Figure 2.2.MIME

GENTLE/s is another end-effector based robot supported rehabilitation system that has been developed in Reading University [6]. GENTLE/s consists of a three DoF robot manipulator named Haptic Master and a virtual reality. In GENTLE/s, the spatial position for the elbow is undetermined, thus two ropes of a weight lifting system is used to compensate the gravity effect. GENTLE/s allows patients to perform 3-dimension point-to-point movements. GENTLE/s system is given in Figure 2.3.



Figure 2.3. GENTLE/s

NeReBot has been designed as a three degrees-of-freedom, wire-driven, end-effector based robot for upper-extremity rehabilitation [7]. There are three wires, which are connected to the patient's upper limbs through a splint, in NeRoBot as shown in Figure 2.4. The rehabilitation treatment based on the passive or active-assistive spatial motion of the limb is provided controlling the lengths of the wires driven by electric motors.



Figure 2.4. NEuroREhabilitationroBOT (NeReBot)

2.1.2. Exoskeleton Type Arm Rehabilitation Robots

ARMin, which has been designed for arm therapy is an exoskeleton robot equipped with position and force sensors [8]. ARMin has four active and two passive DoF to allow elbow flexion/extension and spatial shoulder movements. Later, a second version of ARMin, called ARMin II, has been developed [18]. The mechanical structure, actuators, and sensors of the ARMin has been optimized for the applications of impedance and admittance control for ARMin II. Three therapy modes which are passive mobilization, game therapy, and task-oriented training can be applied to patients with ARMin II. In the latest work, a new ergonomic shoulder actuation principle and its implementation of ARMin II has been developed which is called ARMin III arm therapy robot [19]. Three actuated degrees of freedom for the shoulder and one for the elbow joint are included in ARMin III. Actuated lower arm pronation/supination and wrist flexion/extension are made available with the additional module in ARMinIII. Currently, ARMin III is in use for clinical evaluation in hospitals in Switzerland and United States. ARMin II and ARMin III are shown in Figure 2.5 and Figure 2.6 respectively.



Figure 2.5. ARMin II

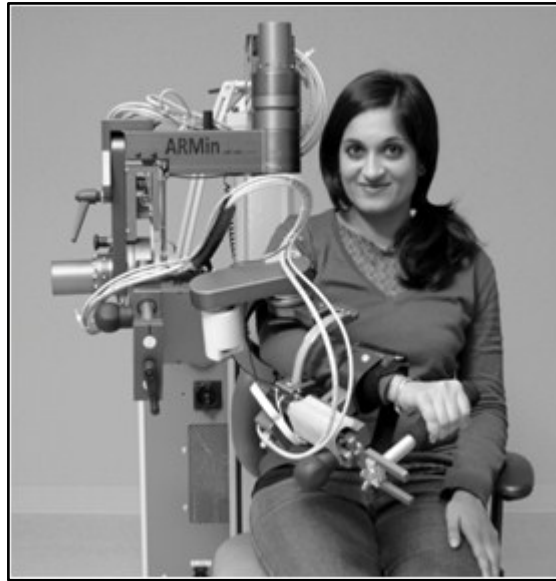


Figure 2.6. ARMin III

The T-WREX (Therapy Wilmington Robotic Exoskeleton) is a passive, five DoF, body powered device with no actuators exoskeleton that has been developed at the University of California Irvine Biomechatronics Laboratory. T-WREX has been designed to enable patients with significant arm weakness to achieve intense movement training without the expense of a physiotherapist [9]. It provides a large 3D workspace that is approximately 66 % of the natural workspace of the arm in the vertical plane and 72 % in the horizontal plane. Weak patients can move their effected arm easily with the support provided against gravity. Pneu-WREX is a robotic version of T-WREX that can apply a wide range of forces to the arm during upper extremity movements using pneumatic actuators [10]. T-WREX is shown in Figure 2.7.



Figure 2.7. T-WREX

L-Exos (Light Exoskeleton) is an exoskeleton robot with force feedback that is designed for right human arm rehabilitation [11]. It has five DoF, four of which are actuated and it can apply a controllable force up to 100 N at the center of the patient's hand palm. L-Exos has active and tunable arm weight compensation. The results of the clinical trials demonstrate that L-Exos can be used for robotic arm rehabilitation therapy when it is integrated with a Virtual Reality (VR) system. The L-Exos system is illustrated in Figure 2.8.



Figure 2.8. L-Exos

The Salford Rehabilitation Exoskeleton (SRE) shown in Figure 2.9 is a gravity compensated arm rehabilitation exoskeleton robot with seven DoF [12]. Three of these DoF are located at the shoulder for flexion/extension, abduction/adduction and

lateral/medial rotation. Two are at the elbow for flexion/extension and pronation/supination of the forearm. The other two provide flexion/extension and abduction/adduction located at the wrist. Pneumatic actuation techniques that provide accurate position and forced controlled paths, compliance and a high level of inherent safety are used in the design of the exoskeleton.



Figure 2.9. SRE

2.2. CONTROL OF ROBOT-ASSISTED REHABILITATION SYSTEMS FOR UPPER EXTREMITIES

Control of a robot assisted rehabilitation system is also an important issue such as its design to complete the rehabilitation task in a desired and safe manner.

MIT Manus uses impedance controller to support the motion of the hand to the target position. MIT-MANUS is back-drivable with low inertia and friction [4]. Thus it is possible to complete the rehabilitation task in a safe manner during the interaction between the patient and the robot. Force and position sensors are used to feed the impedance controller. Position and admittance control strategies are implemented with the six DoF force-torque sensor and position sensors in MIME to execute four different control modes (passive, active-assisted, active constrained and bilateral modes) [5]. GENTLE/s provides assistance to the patients to move to the target points along the predefined trajectories

using the admittance control [6]. Switching Proportional-Integral-Derivative (PID) Control has been used for the position control of NeReBot [7].

Impedance and admittance control techniques have been used for the ARMin robot-assisted rehabilitation systems [8]. Non-linear force control and passive counter balancing techniques have been used for Pneu-Wrex [10]. Impedance control has been used for L-Exos and SRE [11,12].

In this thesis, an admittance control with inner robust position control loop is used to control RehabRoby to provide assistance to the patients. The position control of the joints of RehabRoby is provided by a robust controller with a Kalman filter based disturbance estimator in the proposed controller to minimize the effects of the uncertainties in the dynamics of RehabRoby because of its complex structure [26]. The interaction forces between the subjects and RehabRoby are controlled using admittance control technique. Additionally a high-level controller is designed as a decision making mechanism of RehabRoby using hybrid system modeling technique to monitor the task and assess whether the rehabilitation task or any parameter in the low level controller needs to be updated.

3. METHODOLOGY

First, general control architecture of RehabRoby is presented in this chapter. Then, design specifications and control hardware of RehabRoby are given. Finally, design of the low level and high level controllers of RehabRoby are presented.

3.1. THE CONTROL ARCHITECTURE

A control architecture which is composed of all necessary hardware and software components to complete the rehabilitation tasks in a desired and safe manner, has been developed for robot-assisted rehabilitation system RehabRoby. This control architecture consists of the rehabilitation robot (RehabRoby), low-level and high-level controllers, and a sensory information module. The block diagram of the control architecture is illustrated in Figure 3.1.

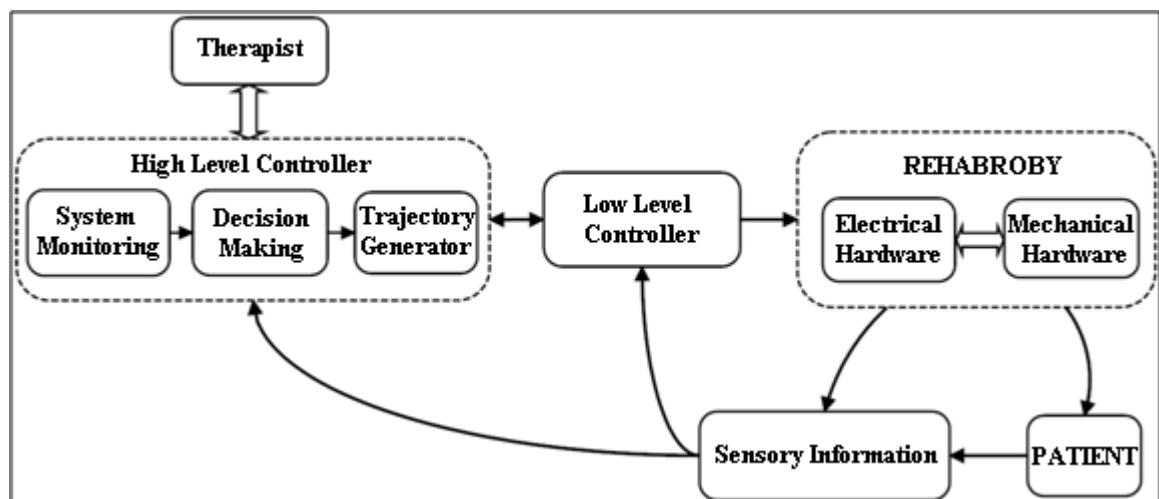


Figure 3.1. Control architecture of RehabRoby

3.2. DESIGN OF REHABROBY

Upper extremity movement characteristics are evaluated during the design phase of RehabRoby. American orthopedic society has provided a standard terminology, which is

based on a consensus on three items, to describe upper extremity movements and movement limits for common clinical examination [20]. First, all positions are referenced on the anatomical posture defined as zero-positions of the joint. Second, joint positions are measured in one of the three (orthogonal) planes (sagittal, frontal or transversal) or around the longitudinal axis (rotation). Finally, the degrees of motion are recorded as the deviation from the reference position in either direction from the anatomical position in a standardized format. Shoulder, elbow and wrist movements according to the standard terminology that are used in rehabilitation and the angles corresponding to these movements are shown in Figure 3.2.

RehabRoby has been designed to provide basic upper extremity rehabilitation movements (extension, flexion, abduction, adduction, rotation, pronation and supination) and also combination of these movements that are necessary for activities of daily living. RehabRoby's motion axes are given in Figure 3.3. Range of motion (RoM), joint torques, velocities and accelerations for RehabRoby have been determined using the measurements of the movements of a healthy subject during two activities of daily living tasks [21,22]. Higher joint torque values than given in [21] and [22] have been selected to assure that RehabRoby will be strong enough to overcome resistance from the human against movements due to spasms and other complications that are difficult to model. These joint torque values are determined by selecting the proper combination of motors and gear units for each joint of RehabRoby. Motion specifications of RehabRoby are given in Table 3.1. Maxon's brushed DC motors, EPOS model drivers (Maxon Motor AG, Switzerland) and gear units of Harmonic Drive (Harmonic Drive Inc., Japan) have been selected for the actuation of the joints of RehabRoby. Basic specifications of the motors, drivers and gear units used in RehabRoby are given in Appendix A. There is a coupling between flexion/extension and abduction/adduction of shoulder axis. The position of the horizontal shoulder rotation angle, which is defined as θ_1 in Figure 3.3, determines the separation of the shoulder movements. When θ_1 is 0^0 , then θ_2 , which represents the position of the flexion/extension and abduction/adduction of shoulder axis as shown in Figure 3.3, is responsible for the flexion/extension of shoulder, and when θ_1 is 90^0 , θ_2 is responsible for the abduction/adduction of shoulder.

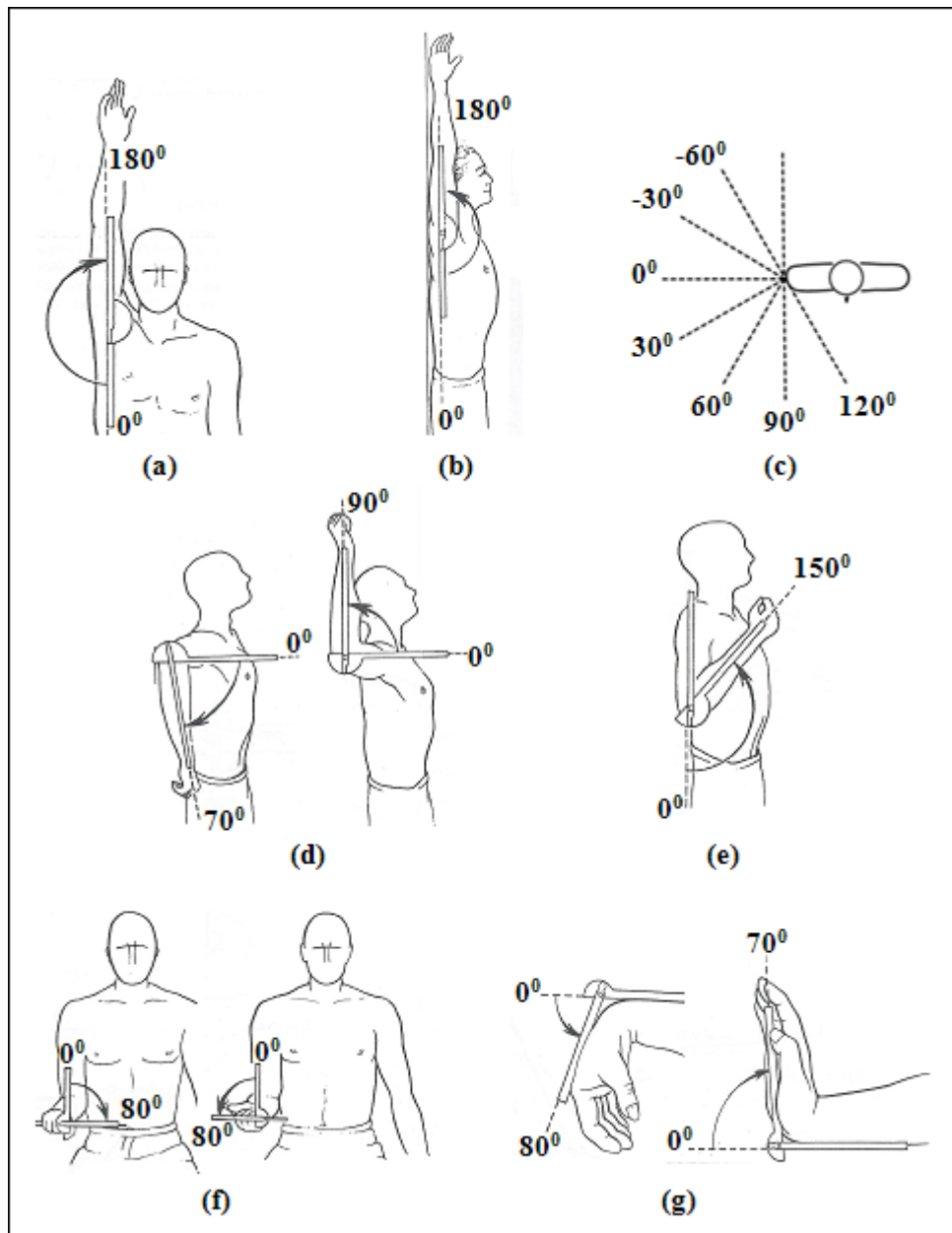


Figure 3.2. Rehabilitation movements for upper extremities and corresponding angle limits, (a) Shoulder abduction and adduction, (b) Shoulder flexion and extension, (c) Angle of the plane of elevation, (d) Internal and external shoulder rotation, (e) Elbow flexion and extension, (f) Lower arm pronation and supination, (g) Wrist flexion and extension.

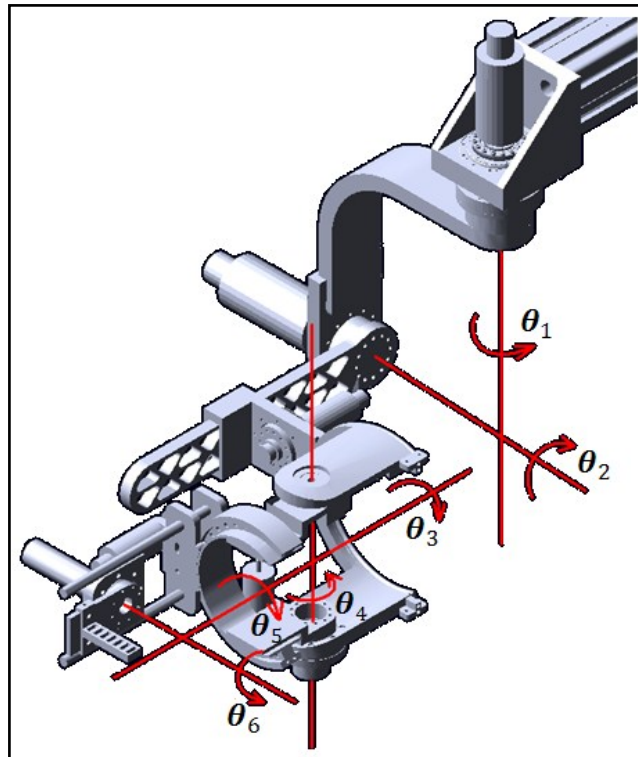


Figure 3.3. RehabRoby's axes, (θ_1 : Horizontal abduction/adduction of shoulder rotation, θ_2 : Shoulder flexion/extension elevation, θ_3 : Internal and external rotation of shoulder, θ_4 : Elbow flexion/extension, θ_5 : Lower arm elbow pronation/supination, θ_6 : Wrist flexion/extension)

Table 3.1. Motion specifications of RehabRoby

Axis	ROM (deg)	Maximum Torque (Nm)	Maximum Velocity (deg/sec)
θ_1	-135°-45°	34.9	332.28
θ_2	-135°-.45°	23.35	447.6
θ_3	-90°-90°	90.44	78.16
θ_4	-90°-30°	34.9	332.28
θ_5	-90°-90°	53.4	72.44
θ_6	-50°-79°	8.5	483

An arm splint has been designed and attached to RehabRoby as shown in Figure 3.4. It has humeral and forearm thermoplastic supports with velcro straps and a single axis free elbow joint. A thermoplastic inner layer covered by soft material (plastazote) is used due to the differences in the size of the subjects' arms. Thus, the total contact between the arm and the splint can be achieved to eliminate loss of movement during the execution of the task.

Ensuring safety of the subject is an important issue when designing a robot-assisted rehabilitation system. Thus, in case of emergency situations, the physiotherapist can press an emergency stop button to stop the RehabRoby. The motor drivers of RehabRoby can be disabled separately or together by pressing the driver enable/disable buttons without disconnecting the energy of the RehabRoby in case of emergency. The power of the system is supported with uninterruptible power supply. Thus, there is no power loss and RehabRoby will not collapse at any time. Additionally, the rotation angle and angular velocity of each joint of RehabRoby are monitored by the high-level controller which will be described in the next section.

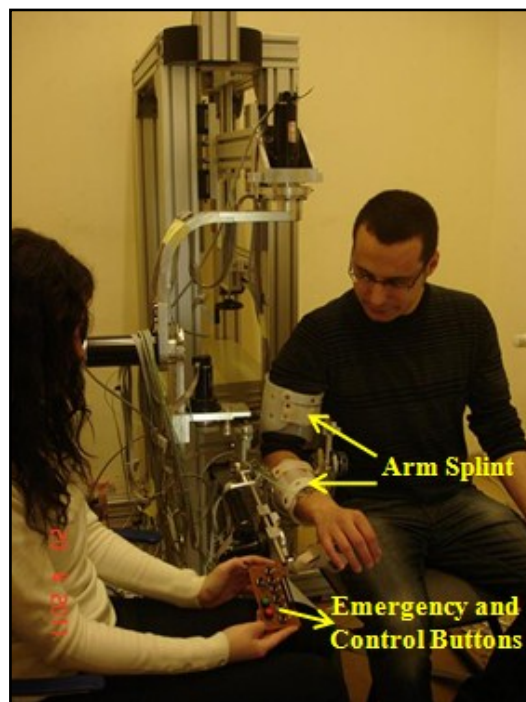


Figure 3.4. RehabRoby system with subject

RehabRoby has been designed in such a way that it can be easily adjustable for people with different heights and arm lengths. In the design of RehabRoby, anthropometric approaches have been used. The link lengths of RehabRoby are based on the arm lengths of 2100 people in 14 cities in Turkey [23]. The adjustable link lengths and height of RehabRoby are shown in Figure 3.5. L_1 which is the adjustable upper arm length value varies from 260 mm to 400 mm. L_2 which is the adjustable lower arm length value varies from 200 mm to 300 mm. Additionally, RehabRoby's height (L_3) can be adjusted for each subject using a screw shaft mechanism that can be manually operated using a wheel. Furthermore, RehabRoby is integrated with a counterweight mechanism as illustrated in Figure 3.6 to reduce the gravity effect to help subjects to flex their shoulders easily. Note that counterweight system is designed in such a way that it does not interfere with the subject's workspace.

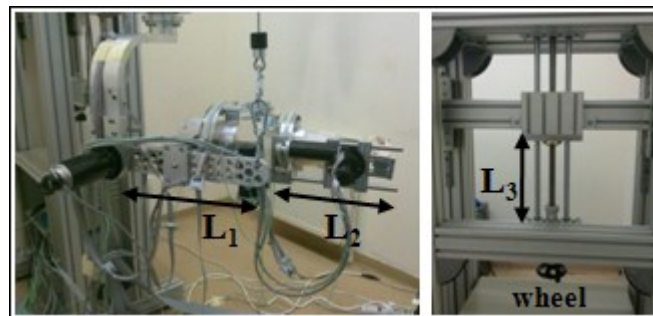


Figure 3.5. Adjustable link lengths and height of RehabRoby

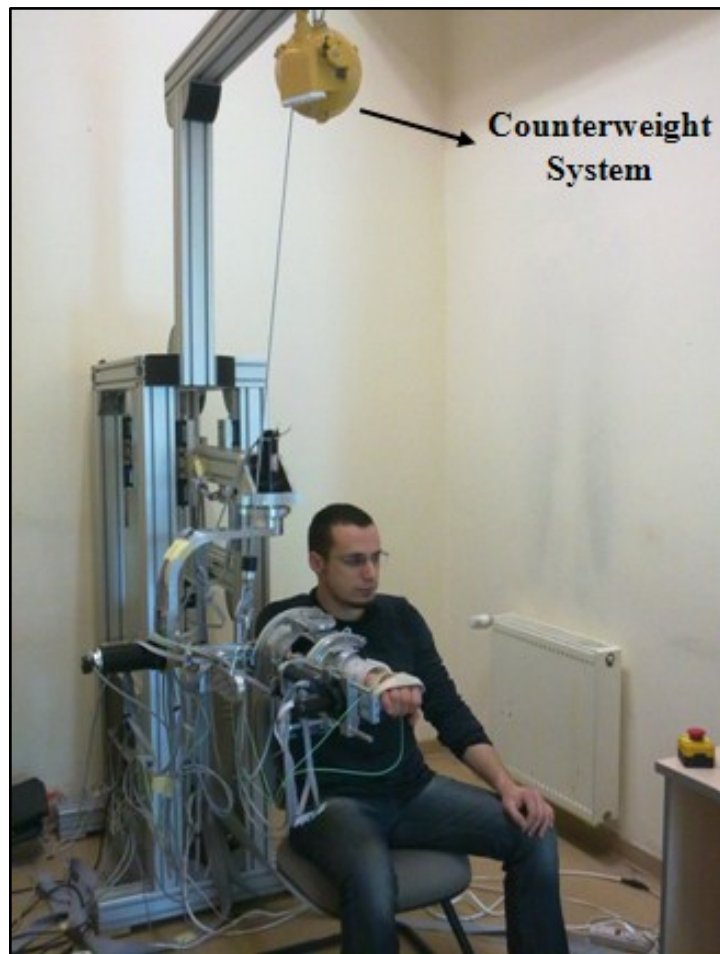


Figure 3.6. RehabRoby with counterweight system

RehabRoby can also be used for both right and left arm rehabilitation. RehabRoby can be translated from right arm use to left arm use with the following steps, i) RehabRoby is rotated 90° about θ_2 , ii) Then RehabRoby is rotated 180° about θ_1 , and iii) RehabRoby is rotated -90° about θ_2 . The transition steps of RehabRoby for left arm use are given in Figure 3.7.

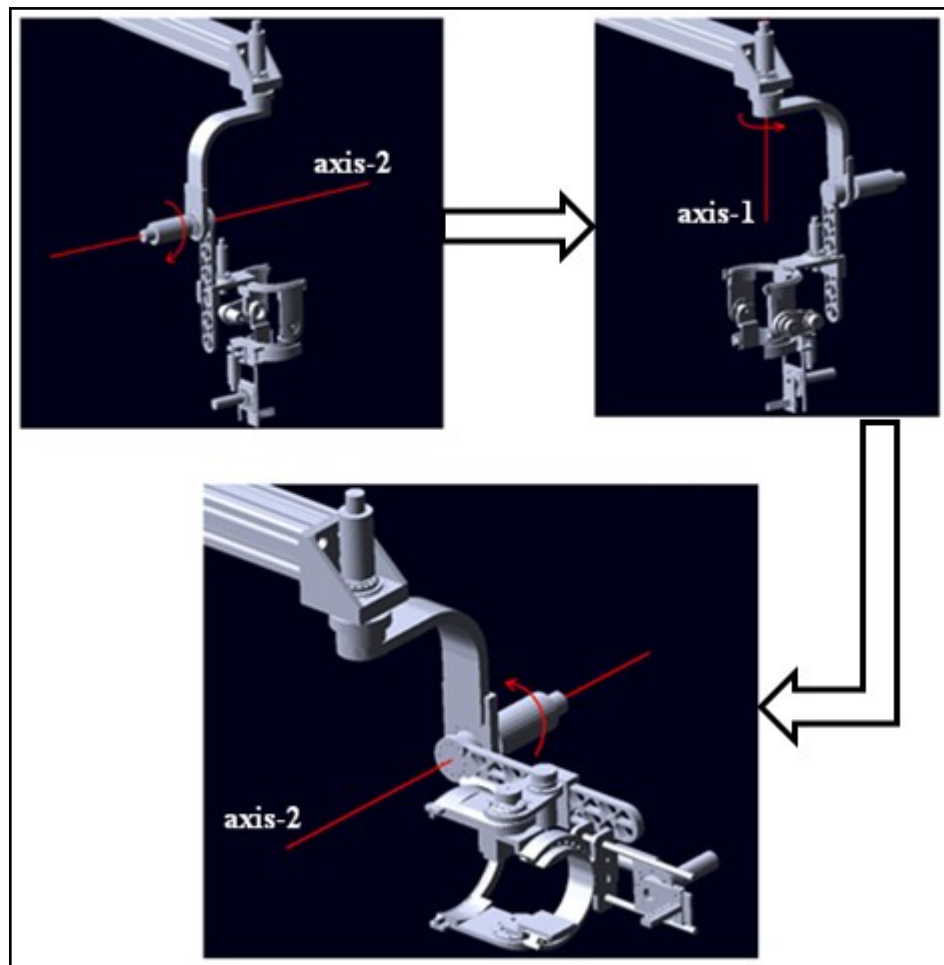


Figure 3.7. Transition steps of RehabRoby for left arm use

3.3. SENSORS AND CONTROL HARDWARE OF REHABROBY

RehabRoby has an interface with Matlab Simulink/Realtime Workshop to allow fast and easy system development. Humusoft Mf624 model (HUMUSOFT Inc., Czech Republic) data acquisition board is selected to provide real time communication between the computer and other electrical hardware. Technical data of this board is given in Appendix B. Humusoft Mf624 data acquisition board is compatible with Real Time Windows Target toolbox of MATLAB/Simulink. Digital incremental quadrature encoders are coupled with brushed DC motors for joint position measurement. Five of the six encoders have resolutions of 500counts/turn and one of them has a resolution of 1000 counts/turn. Kistler's press force sensors (Kistler Holding AG, Winterthur, Switzerland), which have quite small size, are selected to measure contact forces between the subject and

RehabRoby. Detailed information about the force sensors is given in Appendix C. Two force sensors have been placed in the inner surface of the thermoplastic molded plate attached dorsally to forearm splint via velcro straps in such a way that the measurement axes of them are perpendicular to each other. Placement of the force sensors is illustrated in Figure 3.8. One of the force sensors is used to measure the applied force during the elbow flexion movement. The other one measures the applied force during the shoulder flexion movement. Digital encoder data of motors and analog force data come from the force sensors are received through the data acquisition board with 500 Hz sampling frequency.

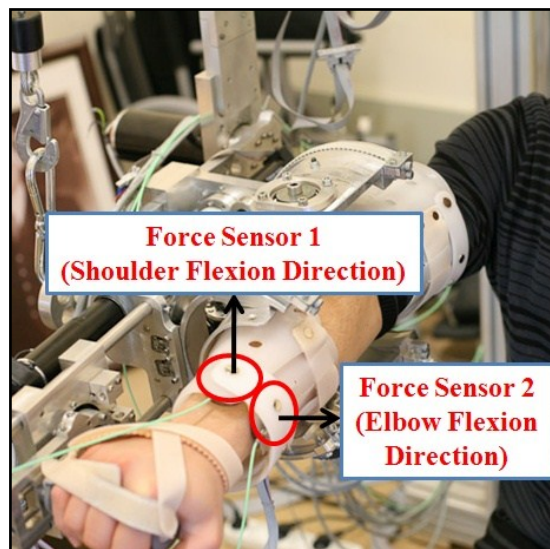


Figure 3.8. Placement of the force sensors

The closed loop data flow in the control hardware occurs between the computer, data acquisition board, microcontroller circuits, motor drivers and motors with encoders. The control inputs which are the current reference values of the motors of RehabRoby are transmitted to the microcontroller circuits through analog outputs of the data acquisition board Humusoft Mf624 with a sampling frequency of 500 Hz. The incoming analog data is converted to digital and transmitted to the motor drivers using RS232 serial bus with 115200 baud by Programmable Interface Controller (PIC) microcontrollers (Microchip Technology Inc., USA) in the microcontroller circuits. Technical data of the microcontroller and the program code are given in Appendix D and Appendix E respectively. Here, microcontroller circuits are used because four of the six motor drivers

of RehabRoby have no analog reference inputs. Analog to digital conversion and serial transmission are completed within two milliseconds. Motor drivers send the reference current values to the motors using a simple current control algorithm to equalize the current values of the motors to the reference ones. Angular changes in the axes are measured by digital encoders coupled with the motors of RehabRoby and transmitted to the MATLAB/Simulink model in computer as feedback through encoder inputs of the data acquisition board Humusoft Mf624. The block diagram of the general data flow in the hardware is shown in Figure 3.9. A 19'' LCD screen is positioned in front of the subject at a distance of about 1 m to display the desired rehabilitation task trajectory and subject's actual movement during the task execution.

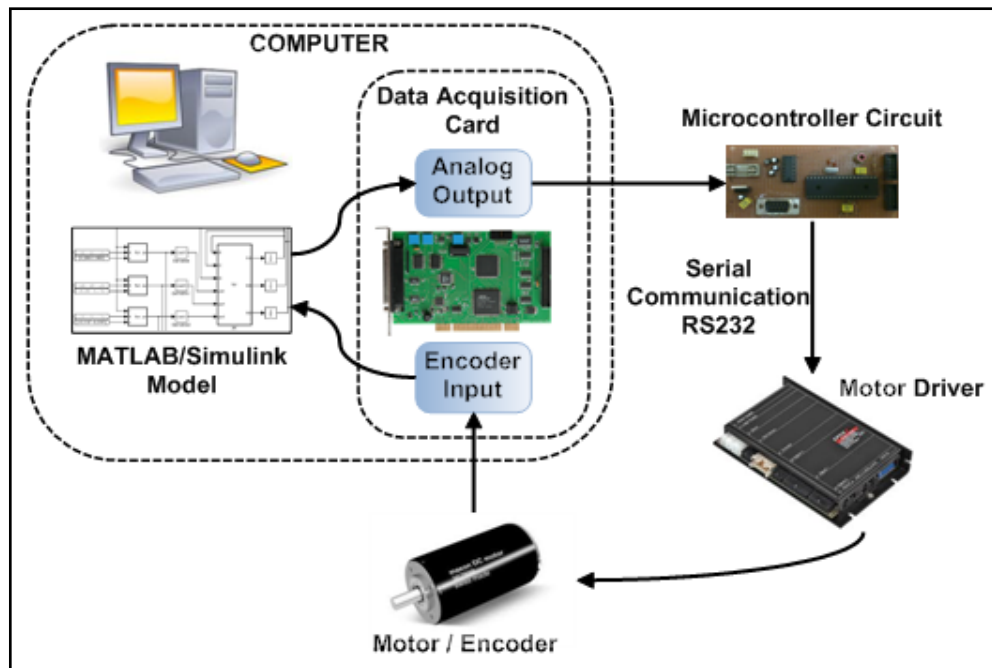


Figure 3.9. General data flow in the control hardware

3.4. CONTROLLERS OF REHABROBY

The control structure of RehabRoby consists of low level and high level controllers. The details of these two controllers will be described in detail in this section.

3.4.1. Low Level Controller

The low-level controller is responsible to provide necessary motion to RehabRoby. Therefore patients can complete the rehabilitation tasks in a desired manner. In this study, admittance control with inner robust position control loop is used as the low-level controller of RehabRoby. The block diagram of low-level controller is given in Figure 3.10. Admittance control method is a good choice for control applications of the robotic systems which have low back drivability, high inertia and reliable position and force/torque information [8]. Additionally, the position and torque sensors of the RehabRoby have high resolutions thus admittance control could be a good choice. Since RehabRoby has complex and uncertain inner dynamics and it is sensitive to external forces during the human-robot interaction, a simple Proportional-Integral-Derivative (PID) or model based position control technique may not be enough to complete. Thus, a robust position controller has been used in the inner loop of the admittance controller. The effects of the parametric uncertainties in the dynamic model and the external additive disturbances are compensated with an equivalent disturbance estimator in this robust position controller. Various methods have been previously used to estimate the disturbance in the position control of robotic systems such as adaptive hierarchical fuzzy algorithm, model based disturbance attenuation [24,25]. In this work, we have used discrete Kalman filter based disturbance estimator, which is a commonly known and successful technique for processing noisy discrete measurements and high-accuracy estimating the unknown states and parameters [26,27]. To our knowledge, admittance control with inner robust position control loop has not been used for control of robot-assisted rehabilitation systems before.

The general structure of the proposed low-level controller for RehabRoby is given in Figure 3.10. The force that is applied by the subject during the execution of the task is measured using the force sensor and this value is then converted to torque using Jacobian matrix. The torque value is then passed through an admittance filter, which is used to define characteristics of the motion of the RehabRoby against the applied forces, to generate the reference motion for the robust position controller [28]. The reference motion is then tracked with a robust position control which consists of a linear Kalman filter based disturbance estimator [26,27].

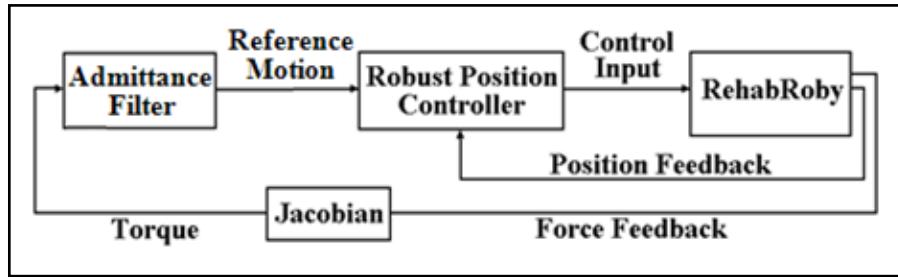


Figure 3.10. Block diagram of low-level controller of RehabRoby

An admittance filter which represents relationship between applied torque and angular change in a joint is represented as:

$$\tau_a = M_d \ddot{q}_r + B_d \dot{q}_r + K_d q_r \quad (3.1)$$

where τ_a , M_d , B_d and K_d represent applied torque, desired inertia, viscosity, and stiffness matrices respectively. q_r , \dot{q}_r ve \ddot{q}_r are reference joint angle, angular velocity and angular acceleration vectors respectively. Equation 3.1 can be represented in s-domain as:

$$q_r(s) = \frac{1}{(M_d s^2 + B_d s + K_d)} \tau_a \quad (3.2)$$

Reference motion is generated by assigning the desired values to M_d , B_d and K_d in the admittance filter and robust position controller in the inner loop is responsible to track the reference motion.

State feedback technique with two feedforward compensation term is used in the robust position control. One of the feedforward terms is used to compensate the modeled RehabRoby dynamics and the other term is used to eliminate the time-varying equivalent disturbances that come from the unmodelled RehabRoby dynamics and unknown external effects. The disturbances are estimated with a recursive algorithm which uses discrete linear Kalman filter (LKF) method [26]. The dynamic equation of robotic systems in joint space is represented as:

$$\tau = M(q)\ddot{q} + V(q, \dot{q}) + b(\dot{q}) + G(q) + \tau_{\text{ext}} \quad (3.3)$$

where τ is the 6x1 joint torque vector, $M(q)$ is the 6x6 manipulator inertia tensor matrix, q , \dot{q} and \ddot{q} are the 6x1 joint position, velocity and acceleration vectors, $V(q, \dot{q})$, $b(\dot{q})$ and $G(q)$ are 6x1 Coriolis and centrifugal, friction and gravity force vectors, respectively. τ_{ext} is the 6x1 torque vector that occurs due to unknown external effects. The inertia tensor $M(q)$ is expressed as:

$$M(q) = \bar{M} + \Delta M(q) \quad (3.4)$$

where the constant diagonal terms of the manipulator inertia tensor $M(q)$ are represented as $\bar{M} = \text{diag}(\bar{M}_1, \bar{M}_2, \dots, \bar{M}_n)$ with $n=1,2,\dots,6$ and the other terms of $M(q)$ are represented in $\Delta M(q)$. Friction term $b(\dot{q})$ is expressed in the same way as in $M(q)$.

$$b(\dot{q}) = B_v \dot{q} + \Delta b(\dot{q}) \quad (3.5)$$

where B_v is the 6x1 viscous-friction coefficient vector. An equivalent disturbance vector d' (6x1), which includes Coriolis, centrifugal and gravity forces, parameter variations in inertia tensor and friction terms, and unknown external effects, is defined as:

$$d' = \Delta M(q)\ddot{q} + V(q, \dot{q}) + \Delta b(\dot{q}) + G(q) + \tau_{\text{ext}} \quad (3.6)$$

If Equation 3.6 is substituted in Equation 3.3, the dynamic equation of RehabRoby is obtained as:

$$\tau = \bar{M}\ddot{q} + B_v \dot{q} + d' \quad (3.7)$$

The relationship between joint torque and the current reference of the actuator is expressed as:

$$\tau = k_t k_{gr} i_r + \Delta \tau \quad (3.8)$$

where k_t is nominal value of the motor torque constant, k_{gr} is the gear ratio of the actuator and i_r is the current reference. $\Delta \tau$ includes both variations of the motor torque constant with respect to its nominal value, k_t , and the variations of the motor current value with respect to current reference value, i_r . Thus total equivalent disturbance d is calculated as:

$$d = d' - \Delta \tau \quad (3.9)$$

The acceleration \ddot{q} is found using $\ddot{q} = (K_{tr}i_r - B_v\dot{q} - d)/\bar{M}$, where K_{tr} is 6x6 diagonal matrix that is calculated by multiplication of k_t and k_{gr} .

The state feedback controller is designed by pole placement. The state space model of the i th joint of RehabRoby as:

$$\dot{x}_i(t) = A_i x_i(t) + B_i u_i(t) + E_i u_{di}(t) \quad (3.10)$$

$$y_i(t) = C_i x_i(t) + v_i(t) \quad (3.11)$$

where $\dot{x}_i(t) = [q_i(t)\dot{q}_i(t)]^T$ is the 2x1 state vector, $u_i(t) = i_{ri}(t)$ is control input (motor current reference), $u_{di}(t) = d_i(t)$ is the equivalent disturbance, $y_i(t) = q_i(t)$ measured output and $v_i(t)$ is the measurement noise. A_i is 2x2 system matrix, B_i is 2x1 control input vector, E_i is 2x1 disturbance vector and C_i is 1x2 output matrix as:

$$A_i = \begin{bmatrix} 0 & 1 \\ 0 & -\frac{B_{vi}}{\bar{M}_i} \end{bmatrix}, B_i = \begin{bmatrix} 0 \\ \frac{K_{tri}}{\bar{M}_i} \end{bmatrix}, E_i = \begin{bmatrix} 0 \\ -\frac{1}{\bar{M}_i} \end{bmatrix}, C_i = [1 \quad 0] \quad (3.12)$$

The control input $u_i(t)$ is selected as:

$$u_i(t) = -K_i x_i(t) + r_i(t) \quad (3.13)$$

where K_i is 1x2 state feedback gain matrix which is described as $K_i = [k_{pi} k_{di}]$. k_{pi} and k_{di} are proportional and derivative gains, respectively. $r_i(t)$ is expressed as follows:

$$r_i(t) = k_{pi}q_{ri}(t) + i_{di}(t) + i_{ci}(t) \quad (3.14)$$

where $q_{ri}(t)$ is reference position for i th joint. $i_{di}(t)$ is the compensating current signal that eliminates equivalent disturbance and calculated using the equation below:

$$i_{di}(t) = \hat{d}_i(t)/K_{tri} \quad (3.15)$$

where $\hat{d}_i(t)$ is estimated value of the equivalent disturbance. $i_{ci}(t)$ is the other feedforward compensating current signal which is calculated as:

$$i_{ci}(t) = (\bar{M}_i/K_{tri})\ddot{q}_{ri}(t) + ((B_{vi}/K_{tri}) + k_{di})\dot{q}_{ri}(t) \quad (3.16)$$

Equation 3.10 with state feedback becomes

$$\dot{x}_i(t) = (A_i - B_i K_i)x_i(t) + B_i r_i(t) + E_i u_{di}(t) \quad (3.17)$$

The characteristic equation of the system defined in Equation 3.17 is represented in s-domain as:

$$s^2 + \frac{1}{\bar{M}_i}(B_{vi} + K_{tri}k_{di})s + \frac{1}{\bar{M}_i}(K_{tri}k_{pi}) = 0 \quad (3.18)$$

Damping ratio (ξ) and natural frequency (ω_0) of the system are calculated using

$$\xi = \frac{B_{vi} + K_{tri}k_{di}}{2\sqrt{\bar{M}_i K_{tri} k_{pi}}} \quad (3.19)$$

$$\omega_0 = \sqrt{\frac{(K_{tri}k_{pi})}{\bar{M}_i}} \quad (3.20)$$

The characteristic time constant of the system is found using $T = (1/\xi\omega_0)$. The control gains k_{pi} and k_{di} for the state feedback control are calculated by assigning desired

values to the ξ , ω_0 and T parameters.

The equivalent disturbance $\hat{d}_i(t)$ is estimated using a recursive algorithm which is based on the linear Kalman filter design. The state space model given in Equation 3.17 is extended by including the estimated equivalent disturbance as a new state variable. The extended model is still linear and time-invariant because equivalent disturbance is independent of state variables [29]. The linear Kalman filter algorithm used in the estimation of the equivalent disturbances is defined in discrete state space. The discrete state space model of i th joint of RehabRoby is described as:

$$x_i(k+1) = (A_{ki} - B_{ki}K_i)x_i(k) + B_{ki}\Gamma_i(k) \quad (3.21)$$

$$y_i(k) = C_{ki}x_i(k) + v_i(k) \quad (3.22)$$

where $x_i(k) = [q_i(k) \dot{q}_i(k) \ d(k)]$ and $r_i(k)$ is expressed as:

$$r_i(k) = k_{pi}q_{ri}(k) + i_{di}(k) + i_{ci}(k) \quad (3.23)$$

The state space matrices of the system defined in Equations 3.21 and 3.22 are given as:

$$A_{ki} - B_{ki}K_i = \left(I + T_s \begin{bmatrix} 0 & 1 & 0 \\ -\frac{K_{tri}k_{pi}}{\bar{M}_i} & -\frac{B_{vi}}{\bar{M}_i} - \frac{K_{tri}k_{di}}{\bar{M}_i} & -\frac{1}{\bar{M}_i} \\ 0 & 0 & 0 \end{bmatrix} \right) \quad (3.24)$$

$$B_{ki} = T_s \begin{bmatrix} 0 \\ \frac{K_{tri}}{\bar{M}_i} \\ 0 \end{bmatrix}, \quad C_{ki} = [1 \ 0 \ 0] \quad (3.25)$$

where T_s is sampling time, which is selected smaller than T. The states at time (k) are predicted using the states estimated at time (k-1) in the discrete linear Kalman filter algorithm using:

$$\hat{x}_i^-(k) = A_{ki}\hat{x}_i(k-1) + B_{ki}u_i(k-1) \quad (3.26)$$

where $\hat{x}_i^-(k)$ is priori estimate of state vector at time (k). The priori estimate value of the 3x3 covariance matrix of estimation errors for the i th joint ($P_i(k)$) is calculated as:

$$P_i^-(k) = A_{ki}P_i(k-1)A_{ki}^T + Q_i \quad (3.27)$$

where Q_i is the 3x3 covariance matrix of model errors. Estimation of the states is updated using the formula below:

$$\hat{x}_i(k) = \hat{x}_i^-(k) + G_i(y_i(k) - C_{ki}\hat{x}_i^-(k)) \quad (3.28)$$

In Equation 3.28, G_i is the 3x1 Kalman gain matrix that minimizes the estimation errors and calculated as:

$$G_i = P_i^-(k)C_{ki}^T(C_{ki}P_i^-(k)C_{ki}^T + R_i)^{-1} \quad (3.29)$$

where R_i is the covariance scalar of measurement error. Covariance matrix of estimation errors $P_i(k)$ is updated as follows:

$$P_i(k) = (I - G_iC_{ki})P_i^-(k) \quad (3.30)$$

Note that the initial values of $\hat{x}_i^-(0)$ and $P_i^-(0)$ are required in the discrete linear Kalman filter algorithm. The block diagram of the robust controller with equivalent disturbance estimation based on linear Kalman filter is shown in Figure 3.11. Asymptotic stability of linear Kalman filter depends on controllability and observability of the system and bounded A, Q and R matrices [30]. Thus, Q_i and R_i are selected as constant matrices and diagonal since the measurement and model noises are considered as stationary random processes.

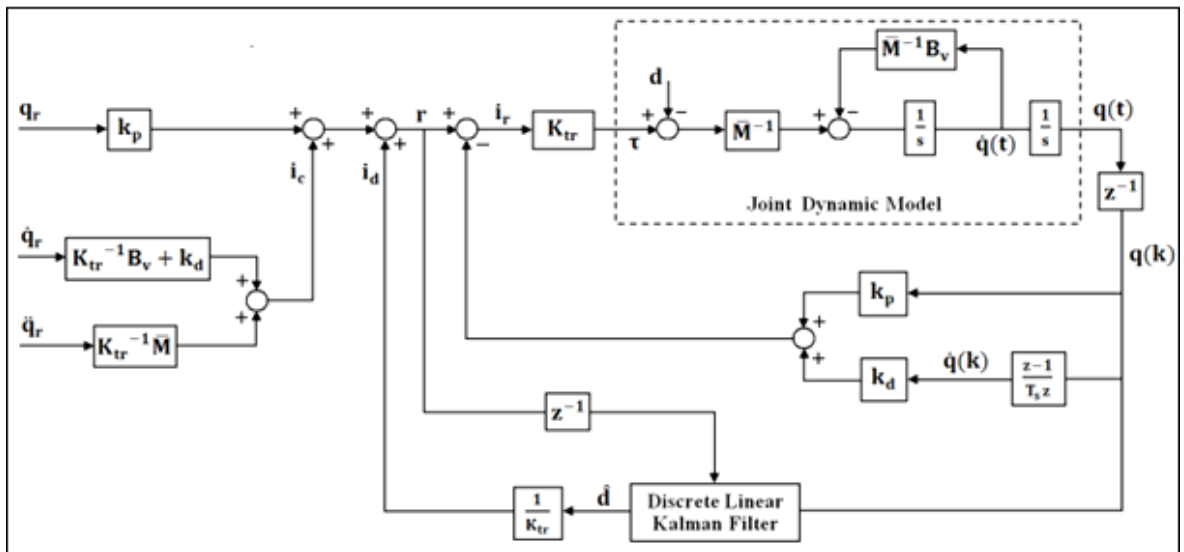


Figure 3.11. Block diagram of the robust position controller with disturbance estimator

3.4.2. High Level Controller

High-level controller is the decision making mechanism of RehabRoby. High-level controller decides necessary changes by analyzing information that comes from the sensory information module or therapist. The high-level controller plays the role of a human supervisor (therapist) who would otherwise monitor the task and assess whether the task needs to be updated. A hybrid system modeling technique is used to design the high-level controller because it is easy to add new rules related to rehabilitation task using this technique Figure 3.12. The block diagram of the high level controller is illustrated in Figure 3.12.

Initially, states of the high-level controller are defined. When task execution starts, starting and final positions of the joint angles of RehabRoby are initialized in *initialization state*. *Passive state (mode=0)* (passive mode), *active state (mode=1)* (active-assisted mode) or *admittance control state (mode=2)* (resistive-assisted mode) become active based on therapist's therapy mode selection. In passive mode, the rehabilitation task is performed only in the passive state in which RehabRoby is responsible to help subject to complete the task when he/she is passive. The subject's motion is checked periodically in active-assisted and resistive-assisted modes. If the subject's movement, which is measured as (θ) of RehabRoby, is out of limits $(\theta \geq |\epsilon|)$, then *position control state* becomes active. When

position control state is active, then RehabRoby provides assistance to subject's motion until subject's movement is in desired motion range. When the subject's movement is in the range of limits ($\theta < |\varepsilon|$), then state, which is active before entering the *position control state*, becomes active again. In any state, safety conditions of RehabRoby are checked periodically and if any unsafe situation occurs ($e=1$), then the *emergency stop state* becomes active and the execution of the task is stopped.

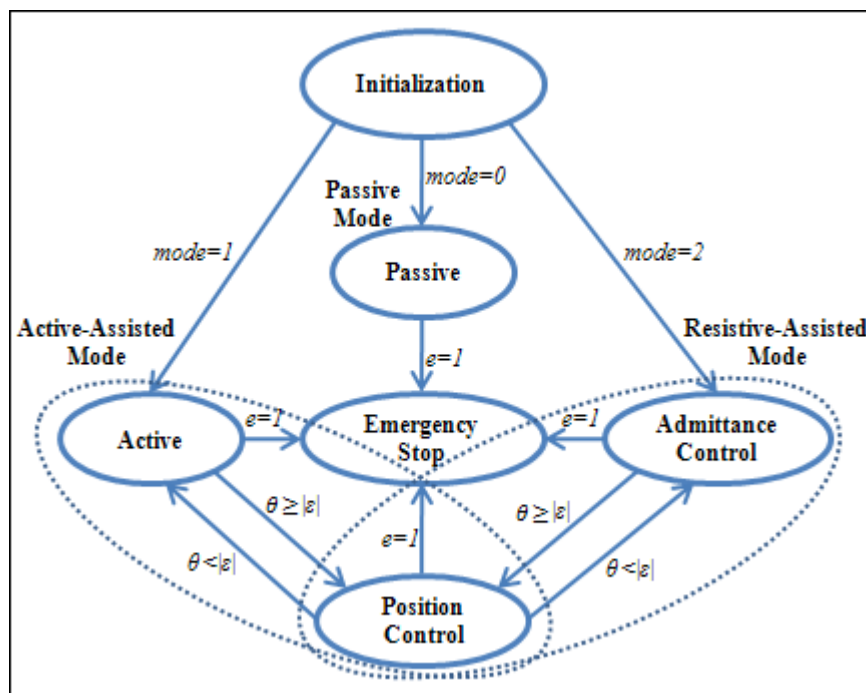


Figure 3.12: Block diagram of the high-level controller of RehabRoby

4. EXPERIMENTAL RESULTS

In this thesis RehabRoby has been evaluated with healthy subjects. The evaluation of the designed control architecture of RehabRoby is presented in detail in this chapter. In the evaluation of the control architecture two well-known rehabilitation tasks are selected in consultation with therapists in Yeditepe University Physical Therapy and Rehabilitation Department. One of the rehabilitation tasks is elbow flexion movement (i.e. reaching towards a glass of water on the table) (Task1) and other one is elbow flexion with shoulder flexion movement (i.e. moving towards to your mouth to eat) (Task2). This study has been approved by Institutional Review Board of Yeditepe University Hospital (IRB #032).

4.1. EXPERIMENTAL PROTOCOL

Subjects were seated in the chair as shown in Figure 3.6 and their arms were placed in the splint tightly secured with Velcro straps. The height of the RehabRoby was adjusted for each subject to start the task in the same arm configuration by changing L_3 shown in the Figure 3.5. Initially, subject's shoulder was positioned at extension of 90^0 , elbow was at neutral position, lower arm was at pronation of 90^0 , and the hand and the wrist were free at neutral position as shown in Figure 4.1. In Task1, subjects were asked to flex their elbows to 90^0 in 30 seconds. In Task2, subjects were asked to flex their elbows to 90^0 and flex their shoulders to 20^0 in 30 seconds.

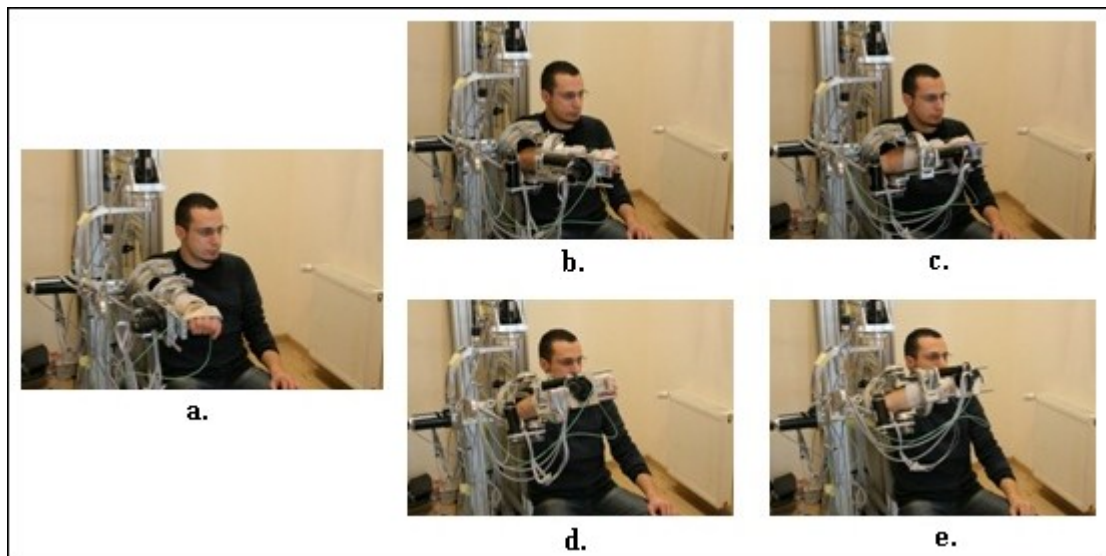


Figure 4.1. Subject with RehabRoby during tasks, a. Initial position of both Task1 and Task2, b. Middle position of Task1, c. Final position of Task1, d. Middle position of Task2, e. Final position of Task2

It is possible for the subjects to perform the rehabilitation tasks in three therapy modes. However, we only selected active-assisted therapy (AAT) and resistive-assisted therapy (RAT) in this study. In AAT, RehabRoby had been kept passive, subjects were asked to perform the tasks by themselves and RehabRoby provided assistance to the subjects when they cannot follow the desired movement. No resistance was applied to the subject's movement in AAT. In RAT, subjects were asked to perform the tasks with a comfortable resistance applied by RehabRoby using admittance control with inner robust position control loop and RehabRoby provided assistance to the subjects when they cannot follow the desired movement. The resistance applied in resistive-assisted mode was quite large compared with the resistance that is caused by inherent dynamics of RehabRoby, thus the resistance of the system in AAT is neglected. The parameters in admittance filter, which provided comfortable resistance, had been determined experimentally. The parameters in admittance filter were selected as $M_d = 4$, $B_d = 3$ and $K_d = 0$ for elbow joint and $M_d = 2$, $B_d = 120$ and $K_d = 0$ for shoulder joint.

9 subjects (4 female and 5 male) whose ages are in the range of 22 to 26 were participated in this study. None of them have any motor impairment in their arms. Two of the subjects were left handed and the others were right handed.

4.2. RESULTS

We initially evaluated performance of the robust position controller with and without discrete linear Kalman filter based disturbance estimator. The approximate values of \bar{M} matrix which includes the mean inertia values corresponding to the each axis of RehabRoby had been calculated experimentally. The i th joint equation of RehabRoby isolated from the effects of the all nonlinear terms and frictions; $K_{tr}i_{ri} = \bar{M}_i\ddot{q}_i(t)$ had been used in the calculations of the values of \bar{M} matrix. The change in the inertia of the i th axis (\bar{M}_i) was observed against an applied constant current and an average inertia value (\bar{M}_i) was calculated by averaging the \bar{M}_i values found in the range where the angular acceleration converged to a fixed value. All average inertia values for each axis of RehabRoby had been calculated with the same way. Viscous friction coefficients had been taken from the datasheets of the motors of RehabRoby. K_{tr} values, which are given in Table 4.1, had been calculated by multiplying torque constants with gear ratios of the joints. The damping ratio ($\xi = 1/\sqrt{2}$) and time constant ($T = 0.4$ seconds) had been used to calculate k_p and k_d . Measurement error covariance R had been selected as 10^{-6} . Model error covariance matrix had been selected as $Q = \text{diag}([10^{-1}10^{-1}10^6])$ and initial values of $\hat{x}^-(0)$ and $P^-(0)$ were taken as zero. Elbow joint (θ_4 -Theta4) of RehabRoby had been flexed to 90° in 10 seconds and subject was asked to stay passive during this movement. Minimum jerk trajectory method was used to define smooth reference motion for elbow flexion movement. Sinusoidal disturbance signal with amplitude of 0.75 and frequency of 2 Hz was added to the reference input, which simulated a situation that might happen during a human-robot interaction. The results of robust position controller with and without discrete linear Kalman filter based disturbance estimator had been presented in Figure 4.2 and Figure 4.3, respectively. When discrete linear Kalman filter based disturbance estimator had not been used, the tracking error had reached about 14° . The state feedback and feedforward compensation signals were not enough for successful trajectory tracking as seen from Figure 4.2. On the other hand, when discrete linear Kalman filter based disturbance estimator estimated the disturbances, the maximum error reduced to 0.70 as seen from Figure 4.3. The equivalent disturbance signal estimated using discrete linear Kalman filter had compensated the effects of the unmodelled parameter variations, nonlinear terms and unexpected external forces. Thus, it is important to design a robust position controller with disturbance estimator for RehabRoby to complete the task

in a safe and desired manner.

Table 4.1. The position controller parameters and RehabRoby model parameters.

Parameter	θ_1	θ_2	θ_3	θ_4	θ_5	θ_6
\bar{M} (kgm ²)	17	10	48	2	30	1
B_v (Nms/rad)	0.0139	0.0379	0.0029	0.0139	0.0014	0.0011
K_{tr} (Nm/A)	3.96	2.77	16.0664	1.98	16.7120	2.59
k_p (A/rad)	53.6778	45.14	37.3563	12.6301	22.4457	4.8277
k_d (A s/rad)	21.4611	18.0369	14.9378	5.0435	8.9755	1.9301

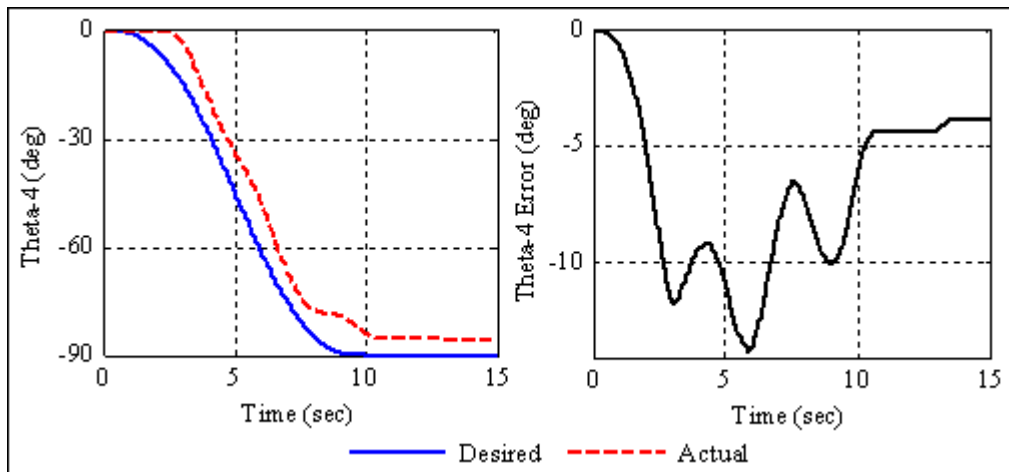


Figure 4.2. Robust position controller without disturbance estimator

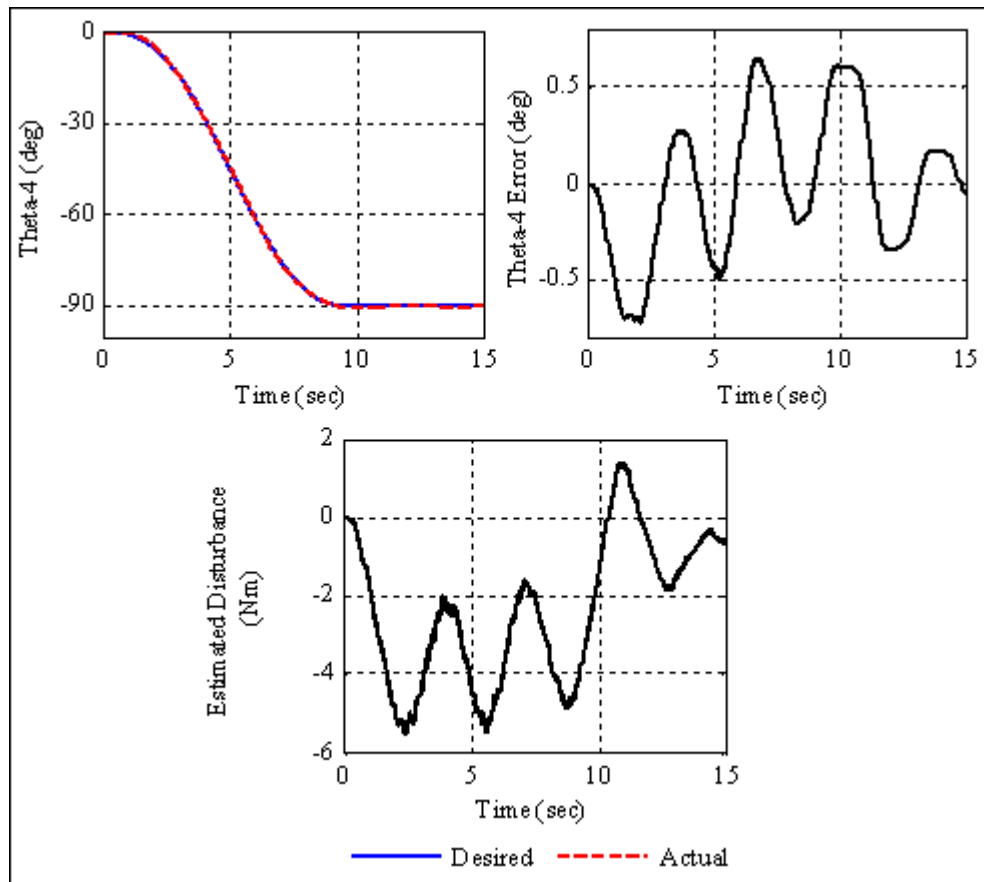


Figure 4.3. Robust position controller with disturbance estimator

We then asked subjects to perform Task1 and Task2 in AAT and in RAT. Subjects were required to move from 0^0 to 90^0 for Task1 and they were asked to trace the green ball shown in Figure 4.4. Actual position of the subject (blue ball), the desired position (green ball) and the desired motion trajectory (black line) were demonstrated to the subjects using a computer screen as shown in Figure 4.4. Upper and lower limits of desired motion of Task1 were shown as perpendicular lines at equal absolute distance from the desired position. Circular area was used to demonstrate limits of the desired motion for Task2.

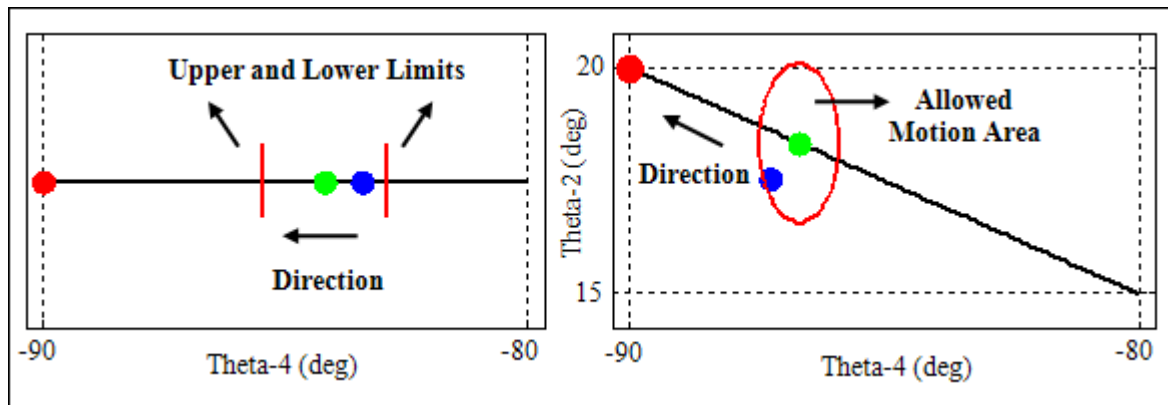


Figure 4.4. Visual feedback, i) Left-Task1, ii) Right-Task2

The subjects were asked to complete Task1 and Task2 using AAT and RAT. Allowed maximum deviation from the reference trajectories was selected as 1.5° . It is possible to increase/decrease the deviation angle depending on the patient's movement capabilities. The subject's movement had been checked in every 2 seconds. If the subject's movement was out of the limits of the desired motion, then RehabRoby became active to provide assistance to the subject to take his/her motion into the desired motion range using robust position controller with disturbance estimator. Experiments were performed with 9 subjects; however we only presented one of the subjects' data (S4 - Subject 4). It could be seen from Figure 4.5 that when the subject was not in the desired motion range, then admittance control with inner robust position control loop became active at time A and the subject came back to the desired motion range at time A'. When the subjects were in the desired range, then the RehabRoby became inactive and subject continued execution of the task by his/her effort. Subject needed more number of times of assistance when he/she had performed Task1 in RAT as shown in Figure 4.6. Same situation had occurred for Task2 as illustrated in Figure 4.7 and Figure 4.8. It had also noticed that transition between the controllers when assistance needed had been smooth as seen from Figure 4.5. Smooth transitions between the controllers during rehabilitation therapies were important to complete the task in a safe manner.

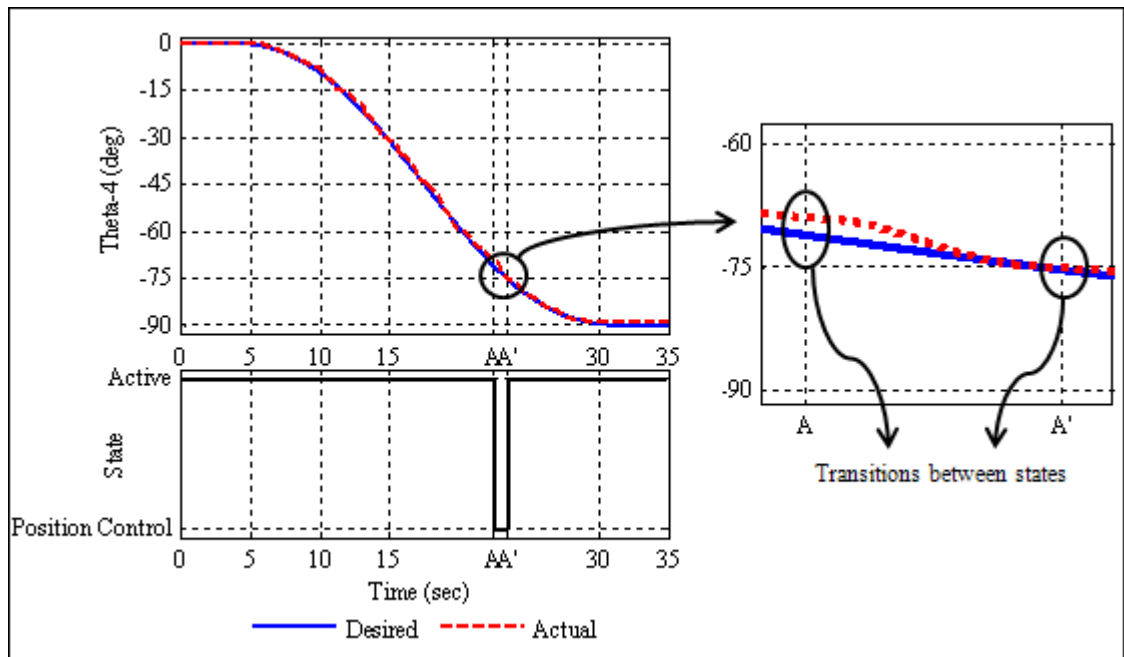


Figure 4.5. Motion of S4 during Task1 in AAT

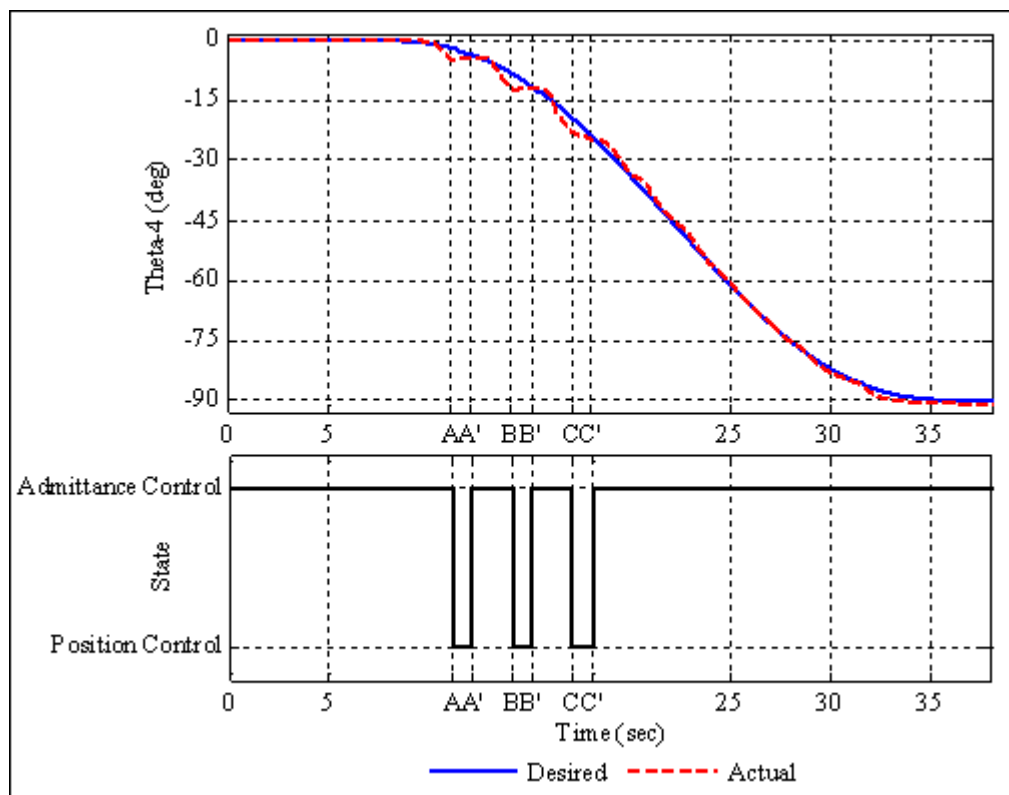


Figure 4.6. Motion of S4 during Task1 in RAT

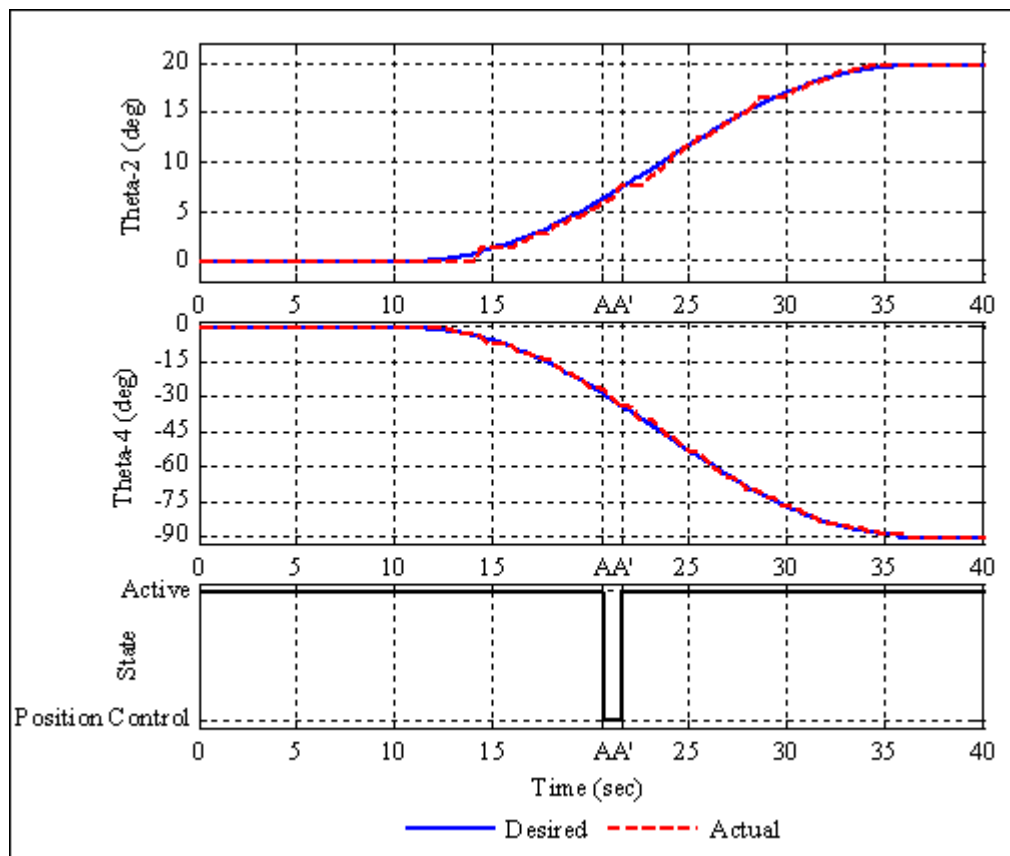


Figure 4.7. Motion of S4 during Task2 in AAT

The position error, which is the difference between the reference and the actual task trajectory, had been calculated for each task. It could be seen from Table 4.2 that the position errors were larger in the RAT than the ones in AAT for both Task1 and Task2. This was because the subjects performed both Task1 and Task2 against a certain resistance in the RAT. The number of times of assistance needed is given in Table 4.3. It was noticed that all subjects except S7 (Subject 7) needed assistance more often when they performed both Task1 and Task2 in RAT. It was because the resistance applied by RehabRoby using the admittance control with inner robust position control loop made both tasks more challenging. Furthermore, most of the subjects needed more number of times assistance when they performed Task2 because Task2 was a two dimensional movement and more challenging task to perform.

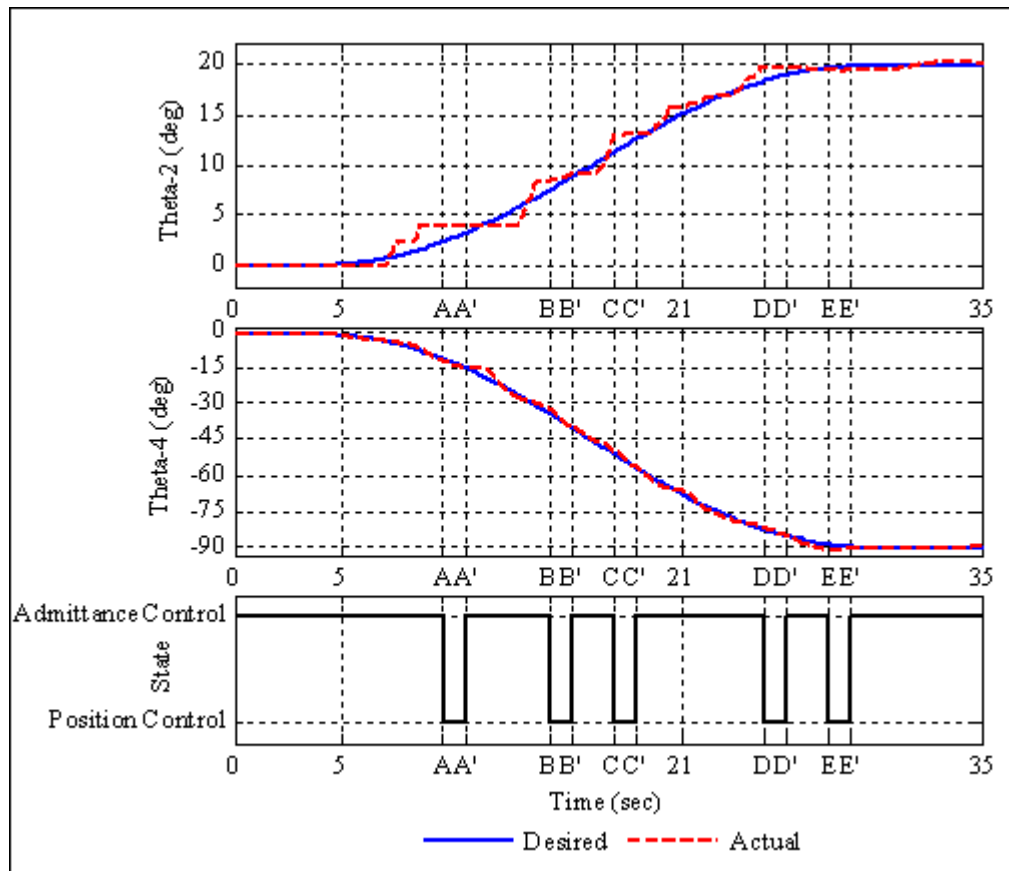


Figure 4.8. Motion of S4 during Task2 in RAT

Table 4.2. Position errors of each subject for both Task1 and Task2

Subjects	Task1 (Deg)		Task2(Deg)			
	AAT	RAT	AAT		RAT	
	θ_4	θ_4	θ_2	θ_4	θ_2	θ_4
S1	0,41	0,58	0,17	0,39	0,47	0,59
S2	0,25	0,33	0,17	0,37	0,39	0,55
S3	0,47	0,74	0,24	0,54	0,43	0,79
S4	0,50	0,87	0,25	0,49	0,50	0,75
S5	0,54	0,77	0,32	0,70	0,45	0,91
S6	0,48	0,70	0,39	0,73	0,69	1,12
S7	0,85	0,98	0,39	0,64	0,47	0,73
S8	0,58	1,22	0,50	0,65	0,48	0,86
S9	0,59	0,79	0,30	0,68	0,42	0,71

Table 4.3. The number of times assistance

Subjects	Task1		Task2	
	AAT	RAT	AAT	RAT
S1	1	1	1	3
S2	1	1	1	3
S3	1	3	2	4
S4	1	3	1	3
S5	2	4	4	6
S6	2	4	4	8
S7	5	4	2	6
S8	1	5	3	5
S9	3	4	3	4

The usability of RehabRoby has been evaluated using a questionnaire. Questionnaire results were presented in Table 4.4.

Table 4.4. Questionnaire results for the assessment of the use of RehabRoby

QUESTIONS	(1) Strongly Disagree	(2) Disagree	(3) Neutral	(4) Agree	(5) Strongly Agree
RehabRoby is a safe system	-	-	0.15	0.40	0.45
RehabRoby can be easily mounted	-	0.15	0.05	0.40	0.40
RehabRoby use is easy	-	0.05	0.15	0.35	0.45
RehabRoby gives fast response to my requests	-	0.5	0.40	0.30	0.25
RehabRoby's speed is suitable	-	0.05	0.15	0.40	0.40
RehabRoby can be used for physical therapy	-	-	0.10	0.35	0.55
I feel no pain after I use RehabRoby	-	0.10	0.15	0.10	0.65
RehabRoby's sensors are comfortable	0.05	-	0.30	0.55	0.10
I am scared when I use RehabRoby	0.90	0.10	-	-	-
I feel tired after performance of the task with RehabRoby	0.55	0.20	0.15	0.10	-

5. CONCLUSION

In this thesis an exoskeleton type upper-extremity robot-assisted rehabilitation system called RehabRoby has been developed. RehabRoby is adaptable for patients with different genders, is adjustable for people with different arm lengths and is usable for both right and left arm.

A control architecture which consists of a high-level controller and a low-level controller has been developed for RehabRoby. High-level controller is the decision making mechanism that decides necessary changes in the low-level controller according to the sensory information or the therapist's commands. A hybrid system modeling technique has been used for high-level controller, which provides flexibility in interfacing low-level controller without extensive redesign cost. Low-level controller is responsible to provide necessary motion to RehabRoby for performing the rehabilitation tasks in a desired manner.

Admittance control with inner robust position control loop, which provides necessary motion to RehabRoby to complete the rehabilitation task in a desired manner, is used. The level of resistance that will be applied by RehabRoby can be varied using admittance control based on the patient's movement capability. Admittance controller has been integrated with a robust position controller which consists of a linear discrete Kalman filter to compensate effects of the parameter variations and nonlinearities in the inherent dynamic model of RehabRoby and the external forces that may happen during the human-robot interaction. When the disturbances are compensated then it becomes possible to control the position of RehabRoby with feedforward and state feedback techniques using robust position controller. We have shown that the tracking error decreased from 14^0 to 0.5^0 when the disturbance estimator was included in the robust position controller. Furthermore, admittance control with inner robust position control loop does not need an exact knowledge of RehabRoby's dynamic model, thus computation effort of the control algorithm has been minimized.

RehabRoby can provide passive, active-assisted and resistive-assisted therapy modes, thus it is possible for low-functioning and high-functioning patients to use RehabRoby in their rehabilitation programs. In the first experiment, two different rehabilitation tasks have been performed using two different therapy modes (active-assisted and resistive-assisted) with healthy subjects to evaluate the control architecture of RehabRoby. Performance of subjects in one dimensional and two dimensional tasks for both therapy modes have been evaluated by calculating the position errors (difference between the reference and subject's actual trajectory). Additionally, the number of times of assistance needed during the execution of both one dimensional and two dimensional rehabilitation tasks has been recorded. The position errors and number of times assistance values have shown that subject's found the tasks more challenging in resistive-assisted mode. Furthermore, subjects found two dimensional task (elbow flexion with shoulder flexion) more difficult than one dimensional task (elbow flexion). It was also noticed that admittance control with inner robust position control provides assistance during the execution of rehabilitation tasks when subjects needed. The transitions between the controllers (when needed) were completed in a smooth manner without causing any nonlinearities and jerks, which is an important issue during execution of the rehabilitation tasks.

In order to include cognitive processing within the rehabilitation tasks, we ask the subjects to follow a visually presented reference motion trajectory that is likely to command their concentration. Subjects are asked to pay attention to tracking the reference trajectory as accurately as possible, which keeps them focused on the task. The visual feedback is used not only to inform the subjects of how closely they are tracking the reference motion but also as a motivational factor to keep them focused on the task. The rehabilitation tasks that are performed by the subjects were designed in such a manner that they required cognitive processing. Including cognitive processing in the task design is an important criterion because it had been previously shown that the movement tracking task that requires cognitive processing achieved greater gains for brain reorganization of stroke patients than that of movement task that does not require cognitive processing [31].

Usability of RehabRoby has been evaluated with a questionnaire. Subjects agreed that RehabRoby is a safe system. Furthermore, subjects thought RehabRoby can be easily

mounted and is easy to use. Additionally subjects found the rehabilitation tasks more difficult when they performed with a resistance.

As a future work, the robust position controller of RehabRoby will be improved using adaptive Kalman filter. Capability of RehabRoby will be extended adding new therapy modes. Note also that this is a feasibility study for the proposed robot-assisted rehabilitation system RehabRoby to be used in the future for rehabilitation of stroke patients.

APPENDIX A: BASIC SPECIFICATIONS OF MOTORS, DRIVERS AND GEAR UNITS USED IN REHABROBY

Basic specifications of the Maxon's brushed DC motors used in the axes of RehabRoby are given in Table A.1.

Table A.1. Basic specifications of motors used in the axes of RehabRoby

Axis / Motors	Nominal Voltage (V)	Nominal Torque (mNm)	Nominal Current (A)	Torque Constant (mNm/A)	Viscous Friction Coefficient (Nms/rad)	Rotor Inertia (gcm ²)
θ_1 / Maxon RE50	24	349	9.04	39.6	0.0139	584
θ_2 / Maxon RE65	24	467	9.23	55.4	0.0379	1290
θ_3 / Maxon RE40	24	170	5.77	30.2	0.0029	138
θ_4 / Maxon RE50	24	349	9.04	39.6	0.0139	584
θ_5 / Maxon RE35	24	93.3	3.36	29.2	0.0014	78.7
θ_6 / Maxon RE30	24	85	3.44	25.9	0.0011	33.3

Maxon's EPOS 24/5 model motor drivers are used for RE35 and RE30 model DC motors and other four motors are driven through Maxon's EPOS 70/10 model drivers. Drivers' specifications are given in Figure A.1.



	<p>EPOS2 24/5</p> <ul style="list-style-type: none"> - DC and EC motors up to 120 W - Point to point control unit (1 axis) - Interpolated Position Mode (PVT) - Combination of several drives via CAN Bus - CANopen - 6 digital inputs (TTL and PLC level) - 4 digital outputs - 2 analog inputs (12-bit ADC) - Compact module design 	<p>Slave version (online commanding) using CAN Master (EPOS2 P, PC, PLC, SoftPLC, etc.) or PC via USB or RS232 interface</p> <p>Typical applications:</p> <ul style="list-style-type: none"> - Tool building - Production equipment - System automation tasks
	<p>EPOS2 70/10</p> <ul style="list-style-type: none"> - DC and EC motors up to 700 W - Point to point control unit (1 axis) - Interpolated Position Mode (PVT) - Combination of several drives via CAN Bus - CANopen - 7 digital inputs (optically isolated) - 3 digital inputs (differential) - 3 digital outputs (optically isolated) - 1 digital output (differential) - 1 digital output - 2 analog inputs (12-bit ADC, differential) - robust design 	<p>Slave version (online commanding) using CAN Master (EPOS2 P, PC, PLC, SoftPLC, etc.) or PC via USB or RS232 interface</p> <p>Typical applications:</p> <ul style="list-style-type: none"> - Production equipment - System automation tasks - Plant construction

Figure A.1. Specifications of the motor drivers

CPU-M model gear units of Harmonic Drive are used with motors in the actuation of the joints of RehabRoby. Rating values of the gear units corresponding to the axis of RehabRoby are given in Table A.2.

Table A.2. Rating Table of Gear Units of RehabRoby

Axis / Gear Unit	Gear Ratio	Limit for Repeated Peak Torque of gear (Nm)	Nominal Output Torque (Nm)	Limit for Momentary Peak Torque (Nm)	Permissible Dynamic Tilting Moment (Nm)	Permissible Dynamic Axial Load (N)	Permissible Dynamic Radial Load (N)
θ_1 / CPU-17-M	1/100	54	24	110	114	4600	2300
θ_2 / CPU-17-M	1/50	34	16	70	114	4600	2300
θ_3 / CPU-14-M	1/100	28	7.8	54	73	2880	1450
θ_4 / CPU-14-M	1/50	18	5.4	35	73	2880	1450
θ_5 / -	-	-	-	-	-	-	-
θ_6 / CPU-14-M	1/100	28	7.8	54	73	2880	1450

APPENDIX B: TECHNICAL DATA OF HUMUSOFT MF624 DATA ACQUISITION BOARD

Humusoft MF624 data acquisition board is shown in Figure B.1.

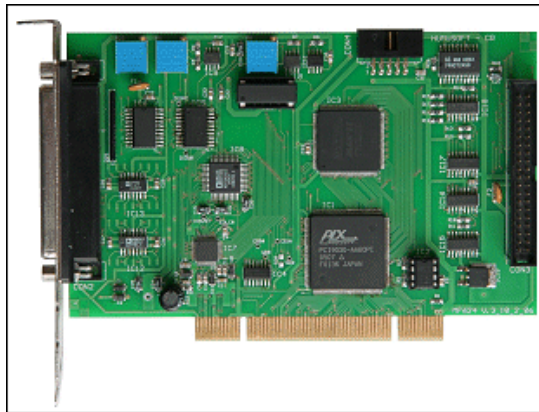


Figure B.1. Humusoft MF624 data acquisition board

Some features and applications of this data acquisition board are as follows:

- 8 single-ended 14-bit analog input channels, Eight 14-bit analog output channels
- Fast conversion rate, low power consumption
- 8 digital inputs, 8 digital outputs, 4 quadrature encoder inputs, 4 counters/timers
- Driver for Real-Time Windows Target
- DC voltage measurement, transducer and sensor interfacing
- Process monitoring and control
- Waveform acquisition and analysis
- Multichannel data acquisition, real-time simulation
- Programmable voltage output
- Position measurements
- Servo systems
- PWM
- Pulse/frequency generation
- Pulse counting

APPENDIX C: CATALOG INFORMATION OF FORCE SENSOR AND ITS CHARGE AMPLIFIER

Technical data of the force sensor and its charge amplifier are given in Figure C.1 and Figure C.2.

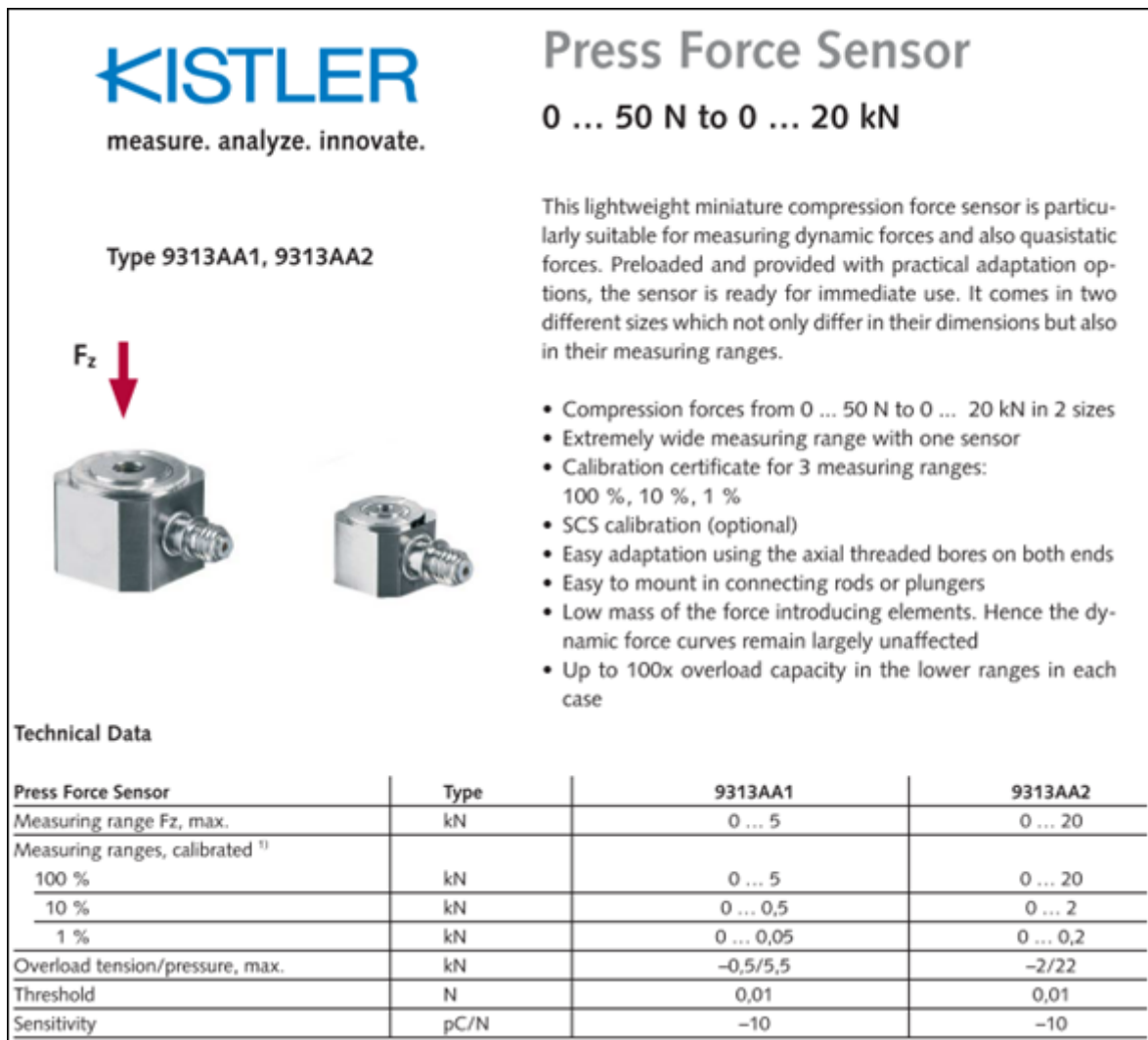


Figure C.1. Technical data of the force sensor

ICAM

Industrial Charge Amplifier for Applications in Manufacturing


The industrial charge amplifier manufacturing (ICAM) converts a charge signal into a low-impedance voltage signal. Depending on version, up to four sensors can be connected at the same time. The ICAM is controlled via digital inputs or the serial interface.

- Wide, variable measuring range $\pm 100 \dots \pm 1\,000\,000$ pC
- Fully configurable via serial interface
- With ManuWare setup and test software
- Industrial models with degrees of protection IP60, IP65 and IP67
- Integrated peak value memory

Technical Data

Versions

Number of channels		1, 2, 3 or 4
Special version		4 charge inputs summed on 1 channel
Alternative input connectors		BNC, TNC
Alternative output signals	V	-10 ... 10
	mA	4 ... 20



Type 5073A...

KISTLER
measure. analyze. innovate.

Figure C.2. Technical data of the charge amplifier

APPENDIX D: TECHNICAL DATA OF THE MICROCONTROLLER (PIC16F877A) USED IN THE MICROCONTROLLER CIRCUIT

Pin diagram of the microcontroller used in the microcontroller circuit is given in Figure D.1.

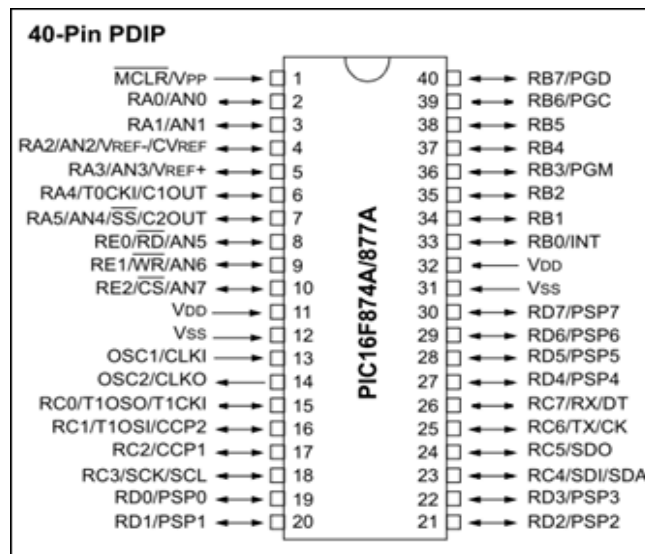


Figure D.1. Pin diagram of the PIC16F877A microcontroller

Basic specifications of PIC16F877A microcontroller are given below:

- All single-cycle instructions except for program branches, which are two-cycle
- Operating speed: DC – 20 MHz clock input, DC – 200 ns instruction cycle
- Up to 8K x 14 words of Flash Program Memory
- Up to 368 x 8 bytes of Data Memory (RAM)
- Timer0: 8-bit timer/counter with 8-bit prescaler
- Timer1: 16-bit timer/counter with prescaler, can be incremented during Sleep via external crystal/clock
- Timer2: 8-bit timer/counter with 8-bit period register, prescaler and postscaler
- Two Capture, Compare, PWM modules
- 10-bit, up to 8-channel Analog-to-Digital Converter (A/D)

APPENDIX E: PROGRAM CODE (IN C LANGUAGE) USED IN THE MICROCONTROLLER

Algorithm E.1. Program code (in c language) used in the microcontroller

```

#include <16F877A.h>
#define ADC=10
#define fuses HS,NOWDT,NOPROTECT,NOLVP
#define use delay(clock=20M)
#define use rs232(baud=115200, xmit=PIN_C6, rcv=PIN_C7)
unsigned int8 e1=0,inter=0,int_count=0,int_count1=0,x=0;
void enable(){
    putc(17);
    putc(3);
    putc(64);
    putc(96);
    putc(0);
    putc(1);
    putc(15);
    putc(1);
    putc(0);
    putc(0);
    putc(230);
    putc(153);
    putc(79);
    putc(79);
    output_high(pin_D0);
    e1 = 1;
}
void disable(){
    putc(17);
    putc(3);
    putc(64);
    putc(96);
    putc(0);
    putc(1);
    putc(0);
    putc(0);
    putc(0);
    putc(0);
    putc(99);
    putc(195);
    putc(79);
    putc(79);
    e1 = 0;
    x=0;
}

```


Algorithm E.1. Program code (in c language) used in the microcontroller (continue)

```

#int_rtcc
void clock_isr() {
    if(inter){
        if(++int_count==50)&&(input(pin_B0)))
            reset_cpu();
    }
    if(e1==0){
        if(++int_count1==38){
            if(x==0){
                output_low(pin_D0);
                x=1;
            }
            else {
                output_high(pin_D0);
                x=0;
            }
            int_count1=0;
        }
    }
}

#int_ext
void isr_x(void){
    disable_interrupts(int_ext);
    inter = 1;
    int_count = 0;
    if (e1==0)
        enable();
    else
        disable();
    enable_interrupts(int_ext);
}

void main() {
    unsigned int16 value,shifter,pdataArray[6],c,carry,CRC=0,
    unsigned int16 crclow,crchigh,valuelow,valuehigh;
    unsigned int8 i=0,e=0,adc_coeff;
    output_low(pin_D0);
    delay_ms(300);
    setup_port_a( ALL_ANALOG );
    setup_adc_ports(AN0);
    setup_adc(ADC_CLOCK_INTERNAL);
    set_adc_channel(0);
    pdataArray[0]=0x1103;
    pdataArray[1]=0x2030;
    pdataArray[2]=0x0100;
    pdataArray[4]=0x0000;
    pdataArray[5]=0x0000;
    set_timer0(0);
    setup_counters(RTCC_INTERNAL, RTCC_DIV_256 | RTCC_8_BIT);
    ext_int_edge(l_to_h);
    enable_interrupts(global);
}

```

Algorithm E.1. Program code (in c language) used in the microcontroller (continue)

```

enable_interrupts(INT_RTCC);
enable_interrupts(int_ext);

while(TRUE){
    while(e1==1){
        if(input(pin_B1)!=e){
            if(input(pin_B2)==0)
                value = read_adc()*adc_coeff;
            else
                value = 65536-read_adc()*adc_coeff;
            pDataArray[3]=value;
            while(i<6){
                shifter = 0x8000;
                c = pDataArray[i];
                do{
                    carry = CRC & 0x8000;
                    CRC <<= 1;
                    if(c & shifter) CRC++;
                    if(carry) CRC ^= 0x1021;
                    shifter>>= 1;
                }
                while(shifter);
                i++;
            }
            valuelow = value&0x00FF;
            valuehigh = value&0xFF00;
            valuehigh = valuehigh>>=8;
            crclow = CRC&0x00FF;
            crchigh = CRC&0xFF00;
            crchigh = crchigh>>=8;
            disable_interrupts(global);
            putc(0x11);
            putc(0x03);
            putc(0x30);
            putc(0x20);
            putc(0);
            putc(1);
            putc(valuelow);
            putc(valuehigh);
            putc(0);
            putc(0);
            putc(crclow);
            putc(crchigh);
            putc(79);
            putc(79);
            e=e^1;
            i=0;
            carry=0,CRC=0,c=0;
            enable_interrupts(global);
        }
    }
}

```

REFERENCES

1. Rehabilitation Research and Training Center on Disability Statistics and Demographics, *Annual Disability Statistics Compendium*, <http://disabilitycompendium.org/Compendium2010.pdf>, 2010.
2. Turkey Disability Survey, *The State Institute of Statistics and The Presidency of Administration*, 2002.
3. Cromwell, S. A. and Owen, P., *Treatment planning in Saunders Manual of Physical Therapy Practice*, R. S. Myers Ed. W.B. Saunders Company, pp.367-374, Philadelphia, 1995.
4. Krebs, H. I., Volpe, B. T., Williams, D., Celestino, J., Charles, S. K., Lynch, D., and Hogan, N., "Robot-Aided Neurorehabilitation: A Robot for Wrist Rehabilitation", *IEEE Transactions on Neural Systems and Rehabilitation Engineering*, Vol. 15, No. 3, September, 2007.
5. Lum, P. S., Burgar, C. G., Van der Loos, H. F. M., Shor, P. C., Majmundar, M., and Yap, R., "MIME Robotic Device for Upper-Limb Neurorehabilitation in Subacute Stroke Subjects: A Follow-Up Study", *Journal of Rehabilitation Research & Development*, Vol.43, pp. 631-642, 2006.
6. Loureiro, R., Amirabdollahian, F., Topping, M., Driessen, B., and Harwin, W., "Upper Limb Mediated Stroke Therapy - GENTLE/s Approach", *Autonomous Robots*, Vol. 15, pp. 35-51, 2003.
7. Rosati, G., Gallina, P., and Masiero, S., "Design, Implementation and Clinical Tests of a Wire-Based Robot for Neurorehabilitation", *IEEE Transactions on Neural Systems and Rehabilitation Engineering*, Vol. 15, No. 4, December, 2007.

8. Nef, T., "ARMin Multimodal Robot for the Movement Therapy of the Upper Extremities", Ph.D. Dissertation, ETH Zürich, citizen of Herisau, AR, 2007.
9. Housman, S. J., Le, V., Rahman, T., Sanchez, R. J., and Reinkensmeyer, D. J., "Arm-Training with T-WREX after Chronic Stroke: Preliminary Results of a Randomized Controlled Trial", *Proceedings of the 2007 IEEE 10th International Conference on Rehabilitation Robotics*, pp. 562-568, Noordwijk, The Netherlands, 2007.
10. Sanchez, R. J., Wolbrecht, E., Smith, R., Liu, J., Rao, S., Cramer, S., Rahman, T., Bobrow, J. E. and Reinkensmeyer, D. J., "A Pneumatic Robot for Re-Training Arm Movement after Stroke: Rationale and Mechanical Design", *Proceedings of the 2005 IEEE 9th International Conference on Rehabilitation Robotics*, pp. 500-504, Chicago, IL, USA, 2005.
11. Frisoli, A., Borelli, L., Montagner, A., Marcheschi, S., Procopio, C., Salsedo, F., Bergamasco, M., Carboncini, M. C., Tolaini, M. and Rossit, B., "Arm Rehabilitation with a Robotic Exoskeleton in Virtual Reality", *Proceedings of the 2007 IEEE 10th International Conference on Rehabilitation Robotics*, pp. 631-642, Noordwijk, The Netherlands, 2007.
12. Kousidou, S., Tzagarakis, N. G., Smith, C. and Caldwell, D. G., "Task-Oriented Biofeedback System for the Rehabilitation of the Upper Limb", *Proceedings of the 2007 IEEE 10th International Conference on Rehabilitation Robotics*, Noordwijk, The Netherlands, 2007.
13. Tsetserukoul, D., Tadakuma, R., Kajimoto, H., Kawakami, N. and Tachi, S., "Towards Safe Human-Robot Interaction: Joint Impedance Control Towards Safe Human-Robot Interaction: Joint Impedance Control", *Proceedings of 16th IEEE International Conference on Robot & Human Interactive Communication*, pp. 860-865, Jeju, Korea, 2007.
14. Krebs, H. I., Ferraro M., Buerger, S. P., Newbery, M. J., Makiyama, A., Sandmann, M., Lynch, D., Volpe, B. T. and Hogan, N., "Rehabilitation Robotics: Pilot Trial of a Spatial

- Extension for MIT-Manus”, *Journal of NeuroEngineering and Rehabilitation*, Vol. 1, pp. 5, 2004.
15. Takahashi, C. D., Der-Yeghiaian, L., Le, V. H., and Cramer, S. C., “A Robotic Device for Hand Motor Therapy after Stroke”, *IEEE 9th International Conference on Rehabilitation Robotics*, pp. 17–20, 2005.
 16. Hesse, S., Wernder, C., Pohl, M., Rueckriem, S., Mehrholz, J. and Lingau, M. L., “Computerized Arm Training Improves the Motor Control of the Severely Affected Arm After Stroke”, *Journal of the American Heart Association*, Vol. 36, pp. 1960-1966, 2005.
 17. Sanchez R., Liu J., Rao S., Shah P., Smith R., Rahman T., Cramer S.C., Bobrow J.E. and Reinkensmeyer D.J., “Automating Arm Movement Training Following Severe Stroke: Functional Exercises With Quantitative Feedback in a Gravity-Reduced Environment”, *IEEE Transactions on Neural Systems and Rehabilitation Engineering*, Vol. 14, No. 3, September, 2006.
 18. Nef, T., Mihelj, M., Kiefer, G., Pemdl, C., Muller, R., Riener, R., “ARMin Exoskeleton for Arm Therapy in Stroke Patients”, *Proceedings of the IEEE 10th International Conference on Rehabilitation Robotics*, Noordwijk, The Netherlands, June 12-15, 2007.
 19. Nef, T., Guidali, M. and Riener, R., “ARMin III - Arm Therapy Exoskeleton with an Ergonomic Shoulder Actuation”, *Applied Bionics and Biomechanics*, Vol. 6, No. 2, pp. 127-142, 2009.
 20. Livingstone, C., *Joint Motion. Methods of Measuring and Recording*, American Academy of Orthopaedic Surgeons, Edinburg, 1965.
 21. Fasoli, S.E., Krebs, H.I. and Hogan, N., “Robotic Technology and Stroke Rehabilitation: Translating Research into Practice”, *Top Stroke Rehabil*, Vol. 11, No. 4, pp. 11-19, 2004.

22. Oldewurtel, F., Mihelj, M., Nef, T. and Riener, R., "Patient-Cooperative Control Strategies for Coordinated Functional Arm Movements", *Proceedings of the European Control Conference*, pp. 2527-2534, Kos, Greece, 2007.
23. Güleç, E., *Anthropometric Dimensions of Human in Anatolia*, T.C. Ankara University Scientific Research Project Report, 2007.
24. Emara, H. and Elshafei, A. L., "Robust Robot Control Enhanced by a Hierarchical Adaptive Fuzzy Algorithm", *Engineering Applications of Artificial Intelligence*, Vol. 17, pp. 187–198, 2004.
25. Choi, C. and Kwak, N., "Robust Control of Robot Manipulator by Model-Based Disturbance Attenuation", *IEEE/ASME Transactions on Mechatronics*, Vol. 8, No. 4, pp. 511-513, 2003.
26. Stasi, S., Salvatore, L. and Milella F., "Robust Tracking Control of Robot Manipulators via LKF-Based Estimator", *Proceedings of the IEEE International Symposium*, pp. 1117-1124, Bled, Slovenia, 1999.
27. Salvatore, L. and Stasi, S., "LKF Based Robust Control of Electrical Servodrives", *IEEE Proceedings Electric Power Appl*, Vol. 3, No. 142, pp. 161-168, 1995.
28. Jung, S. and Hsia, T. C., "Neural Network Impedance Force Control of Robot Manipulator", *IEEE Transactions on Industrial Electronics*, Vol. 45, No. 3, pp. 451-461, 1998.
29. Lee, S. and Ahn, H., "Sensorless Torque Estimation Using Adaptive Kalman Filter and Disturbance Estimator", *Proceedings of IEEE/ASME International Conference on Mechatronics and Embedded Systems and Applications*, pp. 87-92, Qingdao, ShanDong, China, 2010.
30. Gelb, A., Kasper, J. F., Nash, R. A., Price, C. F. and Sutherland, A. A., *Applied Optimal Estimation*, MA: M.I.T. Press, Cambridge, 1988.

31. Carey, J. R., Durfee, W. K., Bhatt, E., Nagpal, A., Weinstein, S. A., Anderson, K. M. and Lewis, S. M., “Tracking vs. Movement Telerehabilitation Training to Change Hand Function and Brain Reorganization in Stroke”, *Neurorehabilitation and Neural Repair*, Vol. 21, pp. 216-232, 2007.